Synthesis of Aib-Pro Oligopeptides by Repeated Azirine Coupling with the Aib-Pro Synthon

by **Svetlana A. Stoykova**[1]), **Anthony Linden**, and **Heinz Heimgartner***

Organisch-Chemisches Institut der Universität Zürich, Winterthurerstrasse 190, CH-8057 Zürich (phone: +41-44-635-4282; fax: +41-44-635-6812; e-mail: heimgart@oci.uzh.ch)

A new synthesis of (Aib-Pro)$_n$ oligopeptides ($n = 2$, 3, and 4) *via* azirine coupling by using the dipeptide synthon methyl *N*-(2,2-dimethyl-2*H*-azirin-3-yl)-L-prolinate (**1b**; *Fig. 1*) is presented. The most important feature of the employed protocol is that no activation of the acid component is necessary, *i.e.*, no additional reagents are required, and the coupling reaction is performed under mild conditions at room temperature. As an attempt to provide an answer to the question of the preferred conformation of the prepared molecules, we carried out experiments by using NMR techniques and X-ray crystallography. For example, in the case of the hexapeptide **11**, it was possible to compare the conformations in the crystalline state and in solution. After the selective hydrolysis of the methyl ester *p*-BrBz-(Aib-Pro)$_4$-OMe (**13**) under basic conditions, the corresponding octapeptide acid was obtained, which was then converted into the octapeptide amide *p*-BrBz-(Aib-Pro)$_4$-NHC$_6$H$_{13}$ (**15**) by using standard coupling conditions and activating reagents (HOBt/TBTU/DIEA) of the peptide synthesis. The conformation of this compound, as well as those of the tetrapeptides **14** and **18**, was also established by X-ray crystallography and in solution by NMR techniques. In the crystalline state, a β-bend ribbon structure is the preferred conformation, and similar conformations are formed in solution.

1. Introduction. – Peptaibol antibiotics, including the well-known alamethicin [2], form an important class of linear peptides of fungal origin, which are characterized by a high content of α,α-disubstituted glycines, *e.g.*, α-aminoisobutyric acid (Aib) and isovaline (Iva), an N-terminal Ac group, and a C-terminal β-amino alcohol [3]. Due to the conformational constraints imposed on the peptide backbone by the presence of α,α-dialkylated glycyl residues, Aib-containing peptides generally form helical structures, either α, 3_{10}, or mixed $\alpha/3_{10}$ helices, depending on the length of the peptide and the number and location of Aib residues [4]. Helix-like structures have also been described in the case of (Aib-Pro)$_n$ oligopeptides and (Xaa-Yaa-Aib-Pro) segments, which give rise to the β-bend ribbon spiral [4a][5], a sub-class of 3_{10}-helices. It has been suggested that the alternation of a conformationally restricted *N*-alkylated amino acid residue such as Pro, which disrupts the conformation-stabilizing H-bonding schemes observed in helices, and a helix-forming residue such as Aib, may give rise to the formation of a β-bend ribbon [4a]. Helical structures are involved in the antimicrobial properties of peptaibols, due to their ability to interact with biological membranes, to modify their permeability and to form voltage-dependent trans-membrane ion channels [6].

---

[1]) Part of the Ph.D. thesis of *S. A. S.*, Universität Zürich, 2004; presented in part at the Autumn Meeting of the Swiss Chemical Society, Lausanne, 2001 [1].

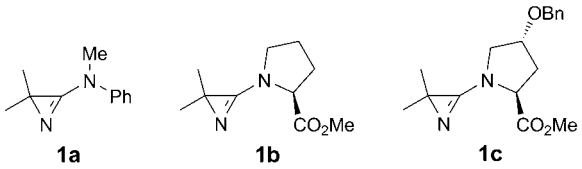

Fig. 1. *2H-Azirin-3-amines as Aib, Aib-Pro, and Aib-Hyp synthons*

Since the discovery of 2,2-disubstituted 2*H*-azirin-3-amines of type **1a** (*Fig. 1*) as synthons for α,α-disubstituted glycines [7], we have reported their use in the synthesis of several peptaibols and peptaibol segments [8], as well as sterically congested model peptides [9], *via* the so-called '*azirine/oxazolone method*'. Furthermore, it has been demonstrated that the building blocks **1** may be used in a modified solid-phase peptide synthesis [8h][10]. The key steps of this method are the spontaneous reaction of an amino or peptide acid **2** with **1a** leading to peptide amides **3** with the backbone extended by an α-methylalanine (Aib), followed by the acid-catalyzed formation of an intermediate oxazolone **4** and coupling of the next amino component to give **5** (*Scheme 1*). Alternatively, under hydrolytic conditions, selective hydrolysis of the intermediates **4** leads to the acids **6**, which can be used for the next '*azirine coupling*'.

Furthermore, methyl *N*-(2,2-dimethyl-2*H*-azirin-3-yl)-L-prolinates **1b** and **1c** have been prepared and found to be suitable as dipeptide synthons for the sequence Aib-Pro and Aib-Hyp (Hyp = 4-hydroxyproline) [8b][11]. These building blocks have been employed in the synthesis of the peptaibol antibiotic trichovirin I 1B and segments of trichovirin I 4A [8b][8e], a segment of zervamicin II-2 [8d], and hypomurocin A1 [8f].

In the present study, we have used the Aib-Pro synthon **1b** for the synthesis of some terminally protected sequential peptides of the type *p*-BrBz-(Aib-Pro)$_n$-OMe, *p*-BrBz-(Aib-Pro)$_n$-NHC$_6$H$_{13}$, and *p*-MeOBz-(Aib-Pro)$_n$-OMe. We also present the results of the conformational studies on these peptides in the solid state and in solution, and the evidence for the β-bend ribbon structure, which has already been reported for analogous peptides with other terminal groups [4a][5].

Scheme 1

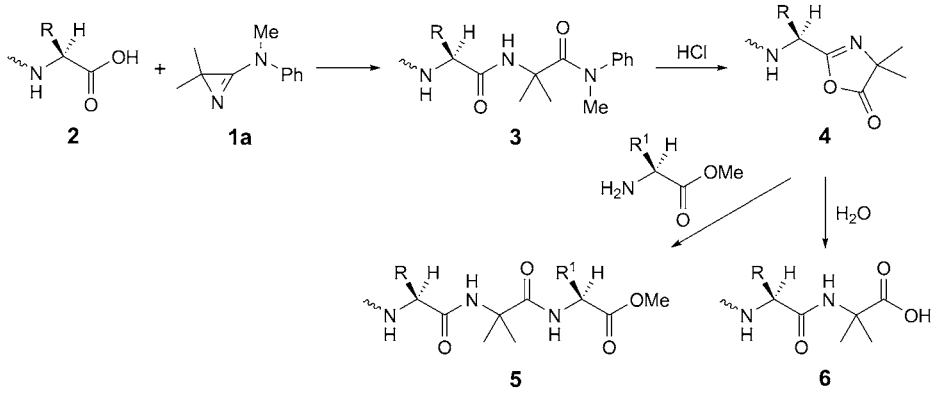

2. Results and Discussion. – 2.1. *Synthesis of the Terminally Protected* p-*BrBz-(Aib-Pro)*$_n$*-OMe and* p-*BrBz-(Aib-Pro)*$_n$*-NHC*$_6$*H*$_{13}$. The dipeptide methyl ester **7** was synthesized in good yield by treatment of 4-bromobenzoic acid (*p*-BrBzOH) with azirine **1b** ('azirine coupling'). A solution of *p*-BrBzOH (1 mol-equiv.) in THF was cooled to 0°, **1b** (1.1 mol-equiv.) was added, and the mixture was stirred for 103 h at room temperature. The product was purified by column chromatography to give **7** in 89% yield (*Scheme 2*). Base-catalyzed hydrolysis of **7** with LiOH · H_2O (4 mol-equiv.) in THF/MeOH/H_2O gave the corresponding dipeptide acid **8** in excellent yield (96%). The isolated product was pure enough to be used in the next coupling with another Aib-Pro unit **1b**. To a solution of **8** (1 mol-equiv.) in CH_2Cl_2 at 0° was added **1b** (1.1 mol-equiv.), and the mixture was stirred for 27 h at room temperature. After chromatographic purification, the tetrapeptide *p*-BrBz-(Aib-Pro)$_2$-OMe (**9**) was obtained quantitatively (99%). Subsequent hydrolysis with LiOH · H_2O (4 mol-equiv.) in THF/MeOH/H_2O afforded the corresponding acid **10** in 93% yield. By repeating the sequence of azirine coupling and hydrolysis, the hexapeptides **11** (ester) and **12** (acid) were prepared in high-to-excellent yields, whereas the azirine coupling of **12** with **1b** furnished the octapeptide ester **13** in only 24% yield.

Scheme 2

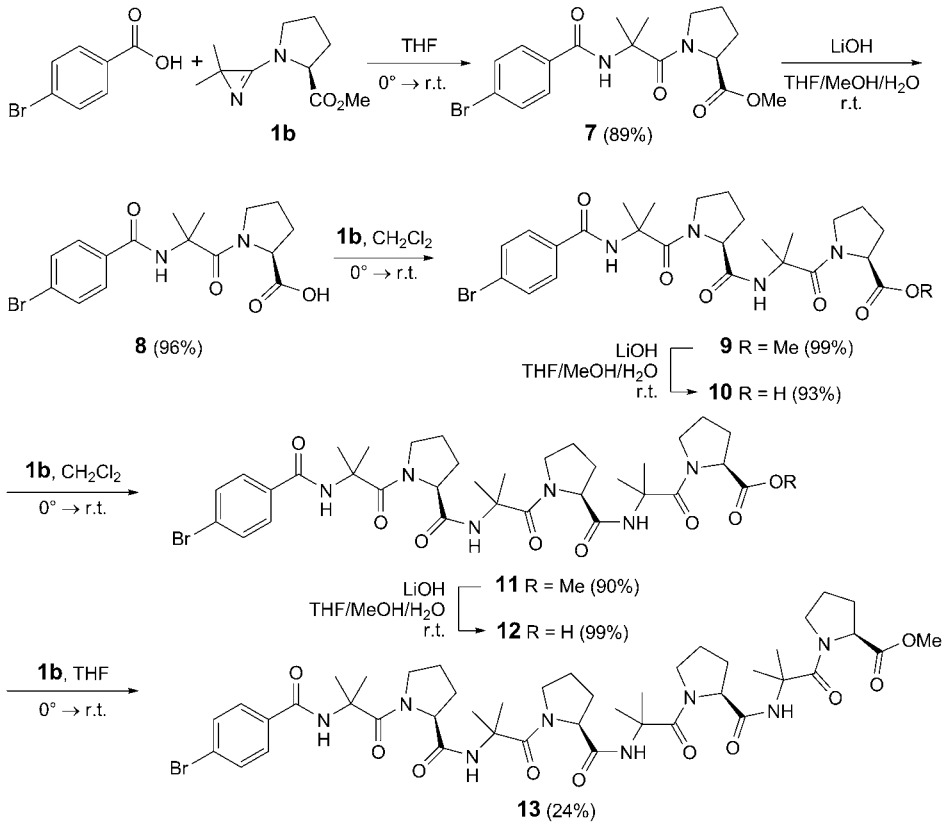

In the case of the hexapeptide ester **11**, suitable crystals for the X-ray crystal-structure determination were obtained by slow evaporation of the solvent from a solution of **11** in CH_2Cl_2/AcOEt. The molecular structure is shown in *Fig. 2*. The absolute configuration (*S*,*S*,*S*) was confirmed independently by the diffraction experiment and agrees with that expected from the synthesis of the compound. The compound contains highly disordered or diffuse solvent molecules. The molecule **11** forms a helix which is held in place in the usual way by two intramolecular H-bonds. N(7)–H and N(13)–H interact with the amide O-atoms that are seven atoms back along the peptide backbone. Each of these interactions has the graph set [12] motif of *S*(10). N(1)–H, which is unable to form an intramolecular interaction because of its position in the backbone, forms an intermolecular H-bond with the amide O(12′)-atom near the middle of a different neighboring molecule. This interaction links the molecules into extended chains which run parallel to the [010] direction and have a graph set motif of *C*(14) (*Fig. 3*). As all possible H-bonds involving the N–H groups have been detected, there are no potential donor interactions with any of the solvent molecules.

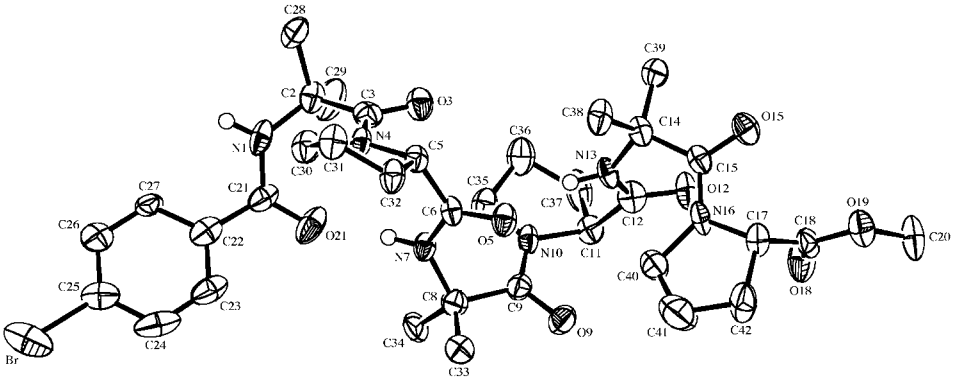

Fig. 2. *ORTEP Plot* [13] *of the molecular structure of* **11** (arbitrary numbering of the atoms; 50% probability ellipsoids; H-atoms bonded to C-atoms omitted for clarity)

Starting with the tetrapeptide acid **10**, the corresponding hexylamide **14** was prepared by a standard peptide-coupling method with 2-[(1*H*-benzotriazol-1-yl)oxy]-1,1,3,3-tetramethyluronium tetrafluoroborate (TBTU) in the presence of 1-hydroxybenzotriazole (HOBt) and (ethyl)(diisopropyl)amine (DIEA, $EtN(i\text{-}Pr)_2$) in CH_2Cl_2 at room temperature (*Scheme 3*). After usual workup, chromatographic purification gave **14** in 90% yield.

Suitable crystals of **14** for the X-ray crystal-structure determination were grown from a solution in CH_2Cl_2 by slow evaporation of the solvent. The molecular structure is depicted in *Fig. 4*. The crystals are enantiomerically pure, and the absolute configuration (*S*,*S*) has been confidently determined independently by the diffraction experiment. The asymmetric unit contains one peptide and two CH_2Cl_2 molecules, one of which is highly disordered. Each N–H group of the peptide molecule acts as a donor for H-bonds. Two of the interactions are intramolecular H-bonds which form a regular

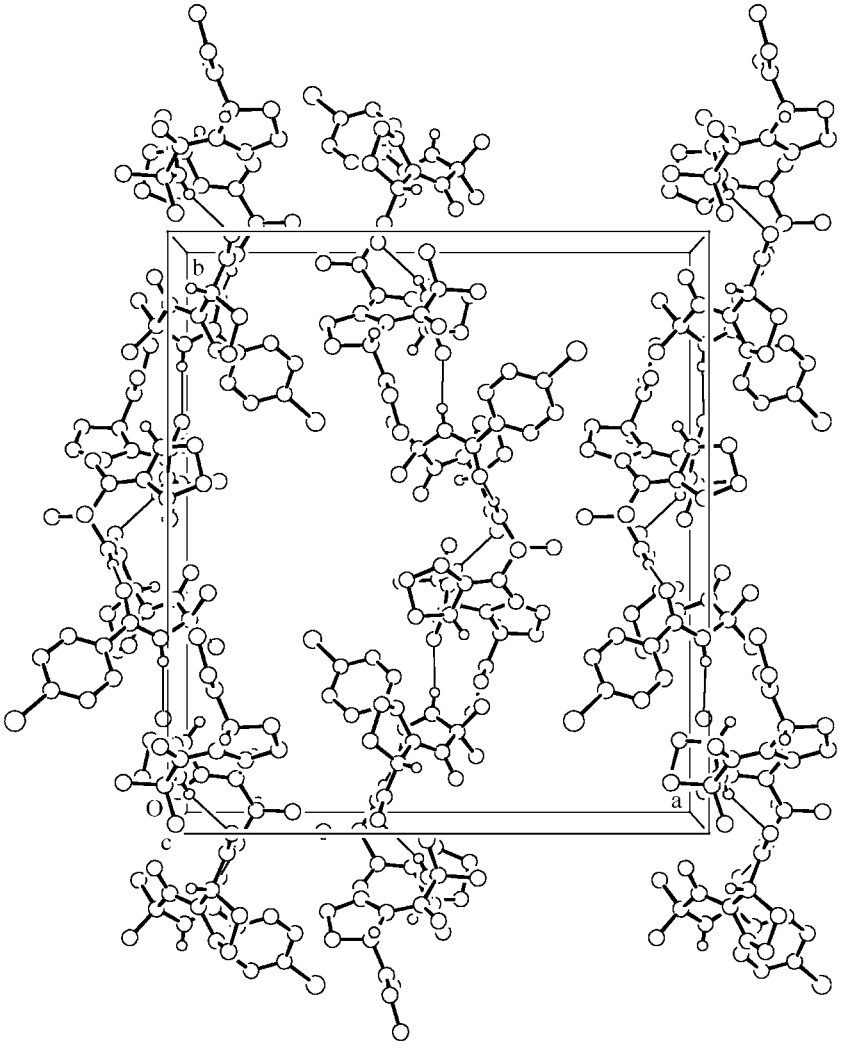

Fig. 3. *Packing diagram of* **11** *showing the H-bonding interactions* (uninvolved H-atoms omitted for clarity)

pattern along the peptide chain and lend the molecule a helical conformation: N(1)–H and N(6)–H interact with the amide O-atoms that are seven atoms further along the peptide backbone. Each of these interactions has the graph set motif of $S(10)$. N(12)–H forms an intermolecular H-bond with the first amide O(1′)-atom at the opposite end of a neighboring molecule. These interactions link the molecules into extended chains which run parallel to the [001] direction and have a graph set motif of $C(14)$ (*Fig. 5*).

In analogy to the sequence **9** → **10** → **14**, the octapeptide ester **13** was transformed into the corresponding hexyl amide **15** (*Scheme 3*). Saponification of **13** with LiOH · H_2O (4 mol-equiv.) in THF/MeOH/H_2O furnished the octapeptide acid in 89% yield,

Scheme 3

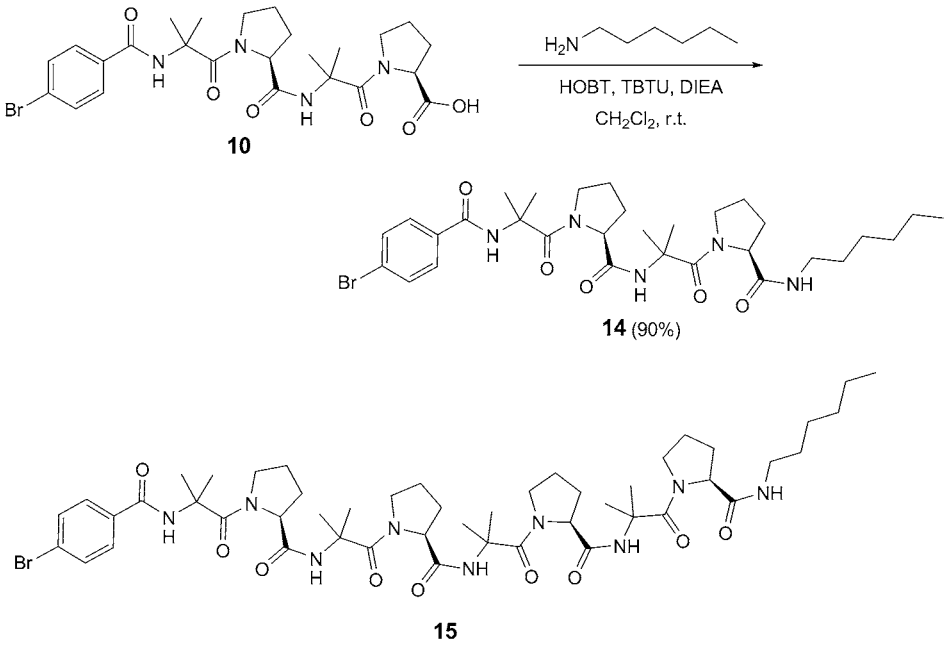

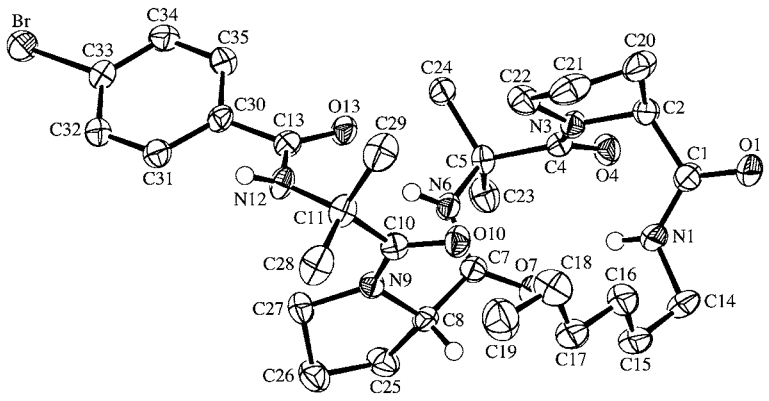

Fig. 4. *ORTEP Plot* [13] *of the molecular structure of* **14** (arbitrary numbering of the atoms; 50% probability ellipsoids; H-atoms bonded to C-atoms and solvent molecules omitted for clarity)

which was reacted with hexylamine by using TBTU/HOBt/DIEA. After chromatographic purification of the crude reaction mixture, the desired octapeptide amide *p*-BrBz-(Aib-Pro)$_4$-NHC$_6$H$_{13}$ (**15**) was obtained in 44% yield.

Crystals of **15** suitable for the X-ray crystal-structure determination were obtained from the mixture CH_2Cl_2/AcOEt/hexane by slow evaporation of the solvent. The molecular structure is shown in *Fig. 6*. The crystals are enantiomerically pure, and the

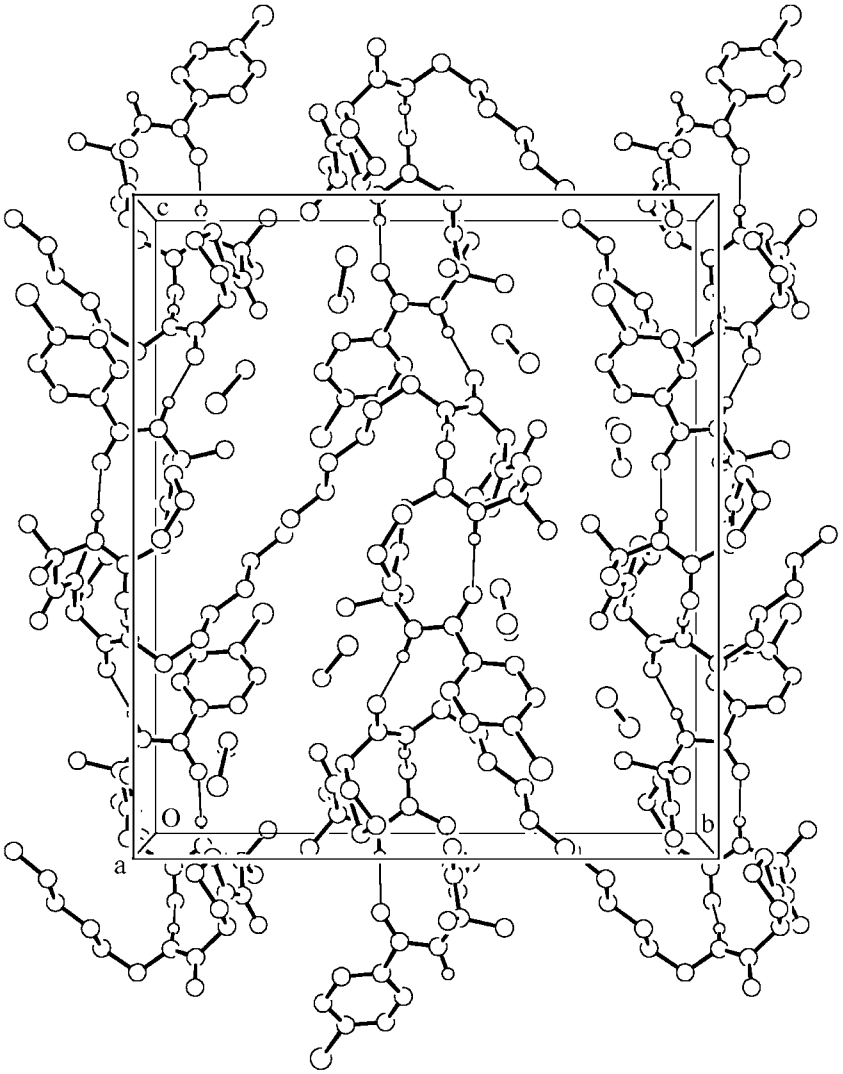

Fig. 5. *Packing diagram of* **14** *showing the H-bonding interactions* (uninvolved H-atoms omitted for clarity)

absolute configuration of the molecule has been confidently determined independently by the diffraction experiment. This confirmed that the compound has the expected (*S*)-configuration at each stereogenic center. The helical conformation of the molecule is controlled by four intramolecular H-bonds. N(1)–H, N(7)–H, N(13)–H, and N(19)–H interact with the amide O-atoms that are seven atoms further along the peptide backbone. Each of these interactions has the graph set motif of *S*(10). N(25)–H, which is unable to form an intramolecular interaction because of its position in the backbone, forms an intermolecular H-bond with the second amide O(5′)-atom from the opposite

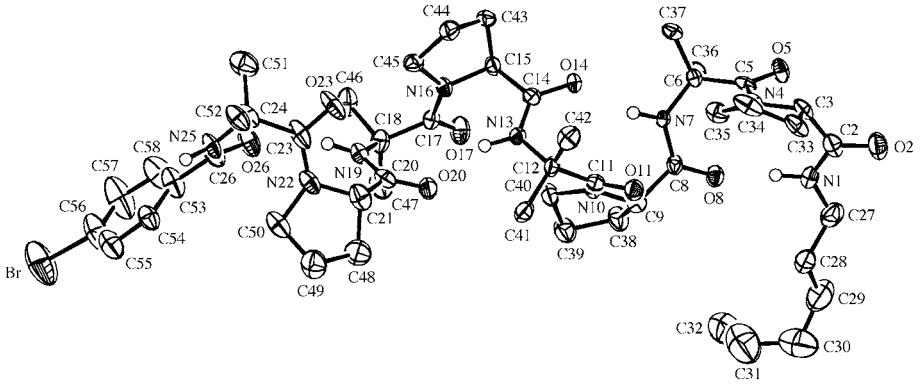

Fig. 6. *ORTEP Plot* [13] *of the molecular structure of* **15** (arbitrary numbering of the atoms; 50% probability ellipsoids; H-atoms bonded to C-atoms omitted for clarity)

end of a neighboring molecule. This interaction links the molecules into extended chains which run parallel to the [110] direction and have a graph set motif of *C*(23) (*Fig. 7*)[2]).

2.2. *Synthesis of the Terminally Protected* p-*MeOBz-(Aib-Pro)*$_n$*-OMe* (**20**). With the aim of studying the potential influence of a MeO group in the *para*-position of the aromatic ring on the peptide structure, we prepared the hexapeptide *p*-MeOBz-(Aib-Pro)$_3$-OMe (**20**) as described in the previous *Sect.* (*Scheme 4*). To a solution of *p*-MeOBzOH (1 mol-equiv.) in THF at 0°, a solution of **1b** (1.1 mol-equiv.) in THF was added, and the mixture was stirred for 42 h at room temperature. After chromatographic purification, the crude dipeptide **16** was obtained as colorless crystals in 85% yield. Saponification of the latter with LiOH · H_2O (4 mol-equiv.) in THF/MeOH/H_2O gave the dipeptide acid **17** in 98% yield. Without further purification, **17** was coupled with **1b** (1.1 mol-equiv.) in CH_2Cl_2 (48 h, r.t.), to afford the tetrapeptide *p*-MeOBz-(Aib-Pro)$_2$-OMe (**18**) in 78% yield.

Suitable crystals for the X-ray crystal-structure determination were obtained by slow evaporation of the solvent from a solution of **18** in $CHCl_3$. The molecular structure is depicted in *Fig. 8*. The asymmetric unit contains one peptide and one highly disordered CH_2Cl_2 molecule plus a site which was assigned to a H_2O molecule with only one quarter site occupancy, although this site lies quite close to the CH_2Cl_2 molecule and may actually be a further disordered position belonging to the CH_2Cl_2 molecule (see *Exper. Part*). The central five-membered ring of the peptide molecule has a disordered envelope conformation in which the envelope flap atom, C(26), flips to either side of the ring. The crystals are enantiomerically pure, however, the absolute configuration of the molecule has not been determined. The enantiomer used in the

---

[2]) Although the conformation of the molecule is clearly defined, the quality and precision of the results are lower than normal, as evidenced by the high *R* factors. This can be attributed to untreated disorder within the molecule. In particular, the alkyl end chain and the bromophenyl group seem to be slightly disordered. However, attempts to model the disorder were unsuccessful, and two significant peaks of residual electron density remain in the vicinity of the Br-atom.

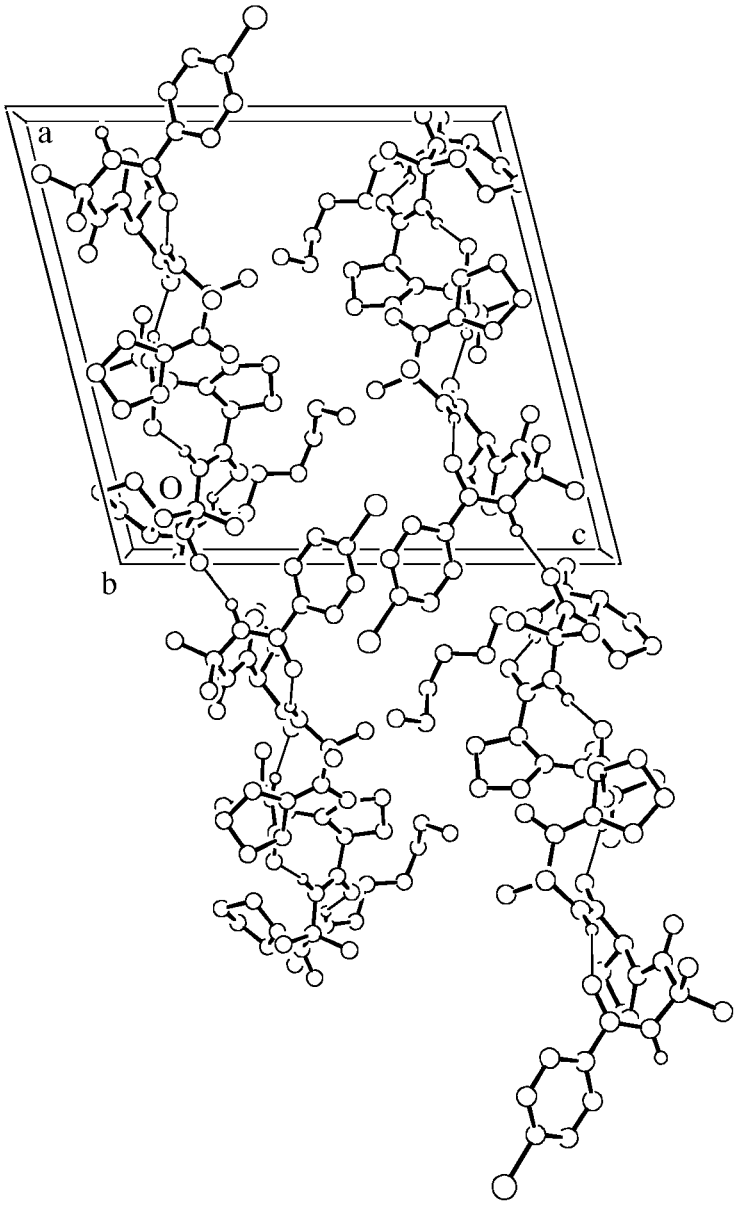

Fig. 7. *Packing diagram of* **15** *showing the H-bonding interactions* (uninvolved H-atoms omitted for clarity)

refinement was based on the known (*S*)-configuration at C(5) and C(11). Each N–H group of the molecule acts as a donor for H-bonds. N(7)–H forms an intramolecular H-bond with the amide O-atom that is seven atoms back along the peptide backbone, thus producing a graph set motif of *S*(10). N(1)–H forms an intermolecular H-bond with the

Scheme 4

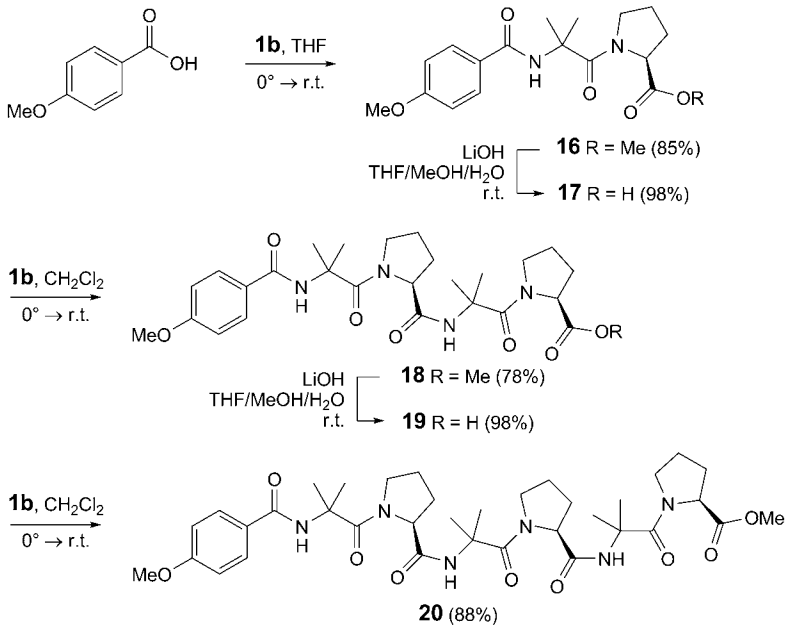

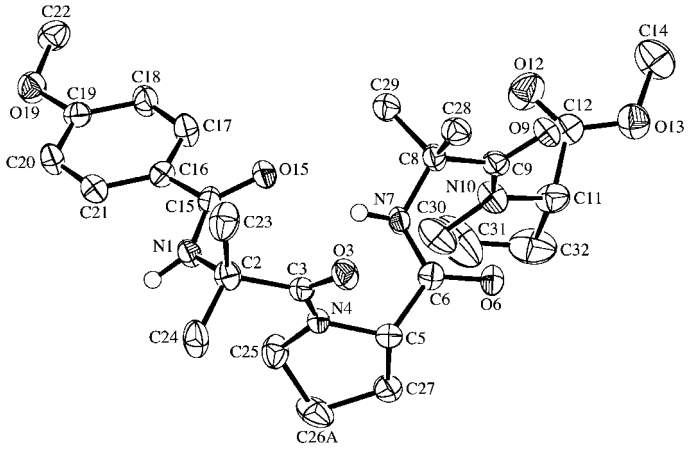

Fig. 8. *ORTEP Plot* [13] *of the molecular structure of one of the two conformers of* **18** (arbitrary numbering of the atoms; 50% probability ellipsoids; H-atoms bonded to C-atoms and solvent molecules omitted for clarity)

second last amide O(9′)-atom from the opposite end of a neighboring molecule. This interaction links the molecules into extended chains which run parallel to the [001] direction and have a graph set motif of $C(11)$ (*Fig. 9*).

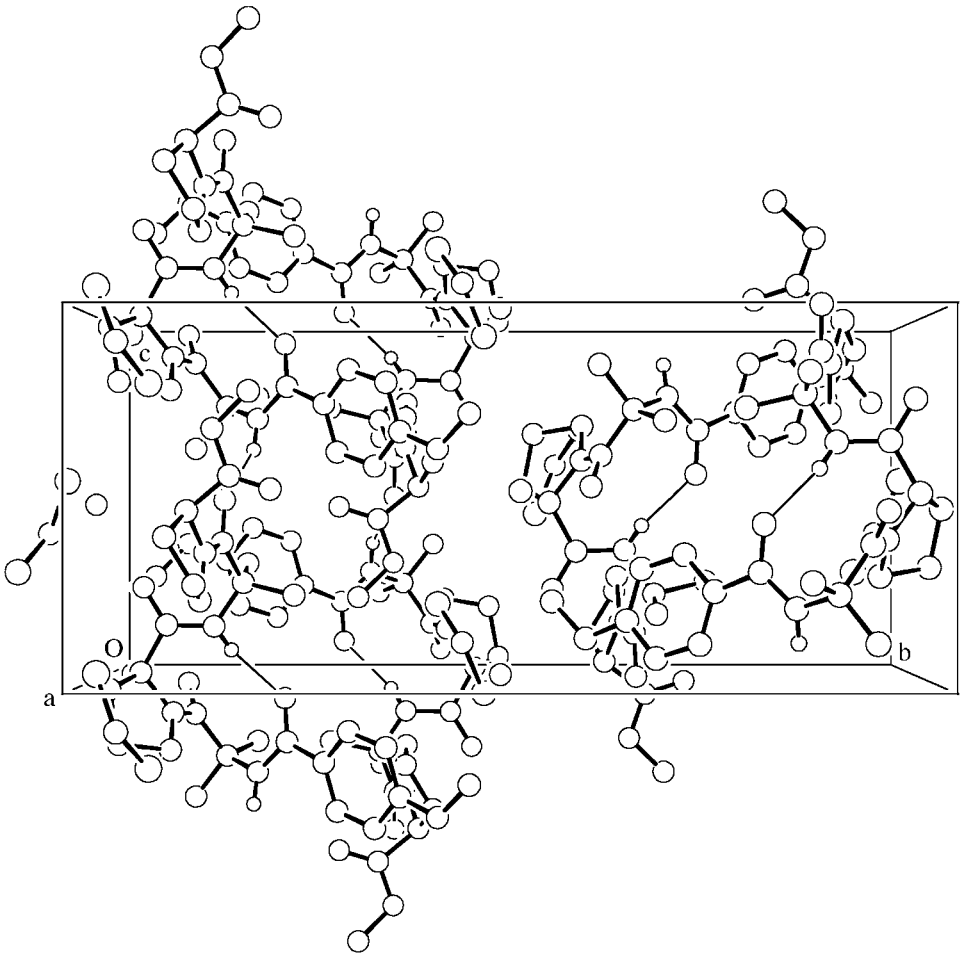

Fig. 9. *Packing diagram of* **18** *showing the H-bonding interactions* (uninvolved H-atoms omitted for clarity; only one conformation of the disordered proline ring is shown)

Basic hydrolysis of **18** under the usual conditions led to the corresponding acid **19** in 98% yield, and the latter was coupled with **1b** to give the hexapeptide *p*-MeOBz-(Aib-Pro)$_3$-OMe (**20**) in 88% yield (*Scheme 4*). Unfortunately, it was not possible to grow suitable crystals for the X-ray crystal-structure determination.

2.3. *Conformational Studies.* 2.3.1. *Octapeptide Amide* p-*BrBz-(Aib-Pro)$_4$-NHC$_6$H$_{13}$* (**15**). The crystal structure and packing of **15** are shown in *Figs. 6* and *7*, respectively. As expected, this molecule shows a helical structure of the β-bend type (see torsion angles of the peptide backbone in *Table 1*). This sub-type of the well-known 3_{10}-helical structure is stabilized by four $1 \leftarrow 4$ intramolecular H-bonds between the NH groups of the Aib(3), Aib(5), and Aib(7) residues, and the NH of the hexylamide moiety and the C=O groups of the *p*-BrBz moiety, and the Pro(2), Pro(4), and Pro(6) C=O groups, respectively (*Table 2*).

Table 1. *Selected Main-Chain Torsion Angles* [°] *of* **15**

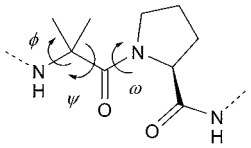

Angle	Aib(1)	Pro(2)	Aib(3)	Pro(4)	Aib(5)	Pro(6)	Aib(7)	Pro(8)
ϕ	– 54.1(6)	– 65.7(5)	– 46.3(5)	– 83.4(4)	– 54.1(5)	– 71.5(4)	– 54.2(5)	– 66.4(4)
ψ	– 30.1(6)	– 5.7(6)	– 42.2(5)	– 7.1(5)	– 29.8(5)	– 12.0(5)	– 39.4(5)	– 16.9(5)
ω	– 175.2(5)	– 179.2(4)	– 170.9(4)	– 175.3(3)	– 173.0(4)	177.6(4)	– 167.9(3)	– 179.9(3)

Table 2. *Intra- and Intermolecular H-Bonds of* **15**

D–H ··· A[a])	D–H [Å]	H ··· A [Å]	D ··· A [Å]	D–H ··· A [°]
N(1)–H(1 ··· O(8)	0.88	2.05	2.856(5)	152
N(7)–H(7) ··· O(14)	0.88	2.05	2.907(4)	165
N(13)–H(13) ··· O(20)	0.88	2.04	2.883(4)	159
N(19)–H(19) ··· O(26)	0.88	2.24	3.070(5)	158
N(25)–H(25) ··· O(5′)	0.88	2.09	2.935(4)	160

[a]) Primed atoms refer to the molecule in the symmetry-related position $1+x$, $1+y$, z.

The Pro side-chain torsion angles of *p*-BrBz-(Aib-Pro)$_4$-NHC$_6$H$_{13}$ (**15**) are compiled in *Table 3*. They show that both C(γ)-*endo* and C(γ)-*exo* pyrrolidine ring puckerings are observed [14]. This finding is in agreement with the results obtained by *Toniolo et al.* who reported that these two pyrrolidine ring conformations have also been observed in the heptapeptide *p*-BrBz-Aib-(Pro-Aib)$_3$-OMe and in the nona-

Table 3. *Pro Side-Chain Torsion Angles* [°] *of* **15**

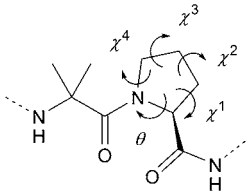

Angle	Pro(2)	Pro(4)	Pro(6)	Pro(8)
θ	4.9(5)	– 14.6(4)	– 1.6(4)	3.3(5)
χ^1	– 25.9(6)	33.1(4)	– 20.4(5)	– 26.1(4)
χ^2	37.1(6)	– 39.1(4)	35.1(5)	39.4(4)
χ^3	– 33.6(6)	29.8(4)	– 35.6(5)	– 36.6(4)
χ^4	17.9(5)	– 9.3(4)	23.4(4)	20.5(5)
Puckering	C(γ)-*exo*	C(γ)-*endo*	C(γ)-*exo*	C(γ)-*exo*

peptide *p*-BrBz-Aib-(Pro-Aib)$_4$-OMe [5c]. These findings rule out the suggestion that this parameter would have a marked effect on the backbone conformation, although some theoretical calculations have shown that the C(γ)-*endo* state is the lowest-energy conformation for the pyrrolidine ring in poly(Aib-Pro)$_n$ peptides, which adopt fairly rigid helical structures stabilized by $1 \leftarrow 4$ intramolecular H-bonds [15].

Information about the three-dimensional structure of the octapeptide *p*-BrBz-(Aib-Pro)$_4$-NHC$_6$H$_{13}$ (**15**) in solution is available from NMR data. A simple indication for the presence of different types of H-bonds is the dependence of the NH shifts on the temperature and on the polarity of the solvent: NH groups involved in intramolecular H-bonds should show a very small dependence, whereas the chemical shifts of solvent-exposed NH H-atoms should be influenced more significantly [16][17]. For the peptide **15**, the involvement of the NH groups in intramolecular H-bonds was evaluated on the basis of the solvent dependence of δ(NH) in $CDCl_3$/(D$_6$)DMSO (solvent-titration experiment [18]) and the temperature dependence. The results obtained from the solvent-titration experiment are presented in *Fig. 10,a*. Four NH groups are almost

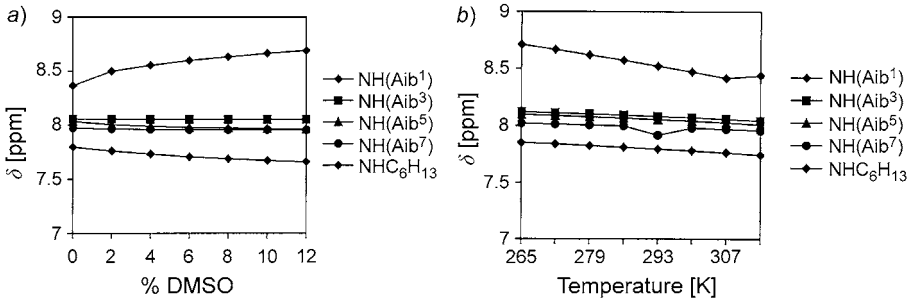

Fig. 10. *Chemical shifts of the NH resonances of* **15** *as a function* a) *of the (D$_6$)DMSO concentration* (in % *v*/*v*) *in CDCl$_3$ and* b) *of the temperature in the range of 265–314 K*

unaffected by an increase of the proportion of (D$_6$)DMSO over the range from 0 to 12%. We assume that these are the NH signals of Aib(3), Aib(5), Aib(7), and the hexylamine moiety, which form four $1 \leftarrow 4$ intramolecular H-bonds as in the crystalline state. The $\Delta\delta$ value of the NH H-atom of the Aib(1) residue is 0.353 ppm, indicating a stronger solvent dependence. The temperature dependence of the NH resonances [19] is displayed in *Fig. 10,b*. The experimentally obtained $\Delta\delta/\Delta T$ values in the temperature range of 265–314 K are collected in *Table 4*. Whereas, the temperature coefficients of NH of Aib(3), Aib(5), Aib(7), and NHC$_6$H$_{13}$ are small (-1.66 to -2.33×10^{-3} ppm/K), the coefficient of the NH H-atom of Aib(1) is -7.46×10^{-3} ppm/K, which could be interpreted as the result of the solvent exposure of this NH H-atom. From these results, it can be concluded that **15** adopts in solution a helical structure analogous to that in the crystal.

2.3.2. *Octapeptide Ester* p-*BrBz-(Aib-Pro)$_4$-OMe* (**13**). As crystals of **13** suitable for X-ray crystallography could not be obtained, ^{1}H-NMR solvent-titration experiments were carried out, and the temperature dependence of the NH absorptions was

Table 4. *Temperature Coefficients* ($-\Delta\delta/\Delta T$ [ppm/K]) *for Amide NH of the Peptides* **15**, **13**, **11**, **14**, *and* **18** *in the Range of 265–314 K*

	NH(Aib(1))	NH(Aib(3))	NH(Aib(5))	NH(Aib(7))	$NH(C_6H_{13})$
15	-7.46×10^{-3}	-1.66×10^{-3}	-1.88×10^{-3}	-2.40×10^{-3}	-2.23×10^{-3}
13	-10.20×10^{-3}	-1.82×10^{-3}	-1.16×10^{-3}	-1.44×10^{-3}	–
11	-10.55×10^{-3}	-1.60×10^{-3}	-1.02×10^{-3}	–	–
14	-10.58×10^{-3}	-2.80×10^{-3}	–	–	-2.73×10^{-3}
18	-12.10×10^{-3}	-3.89×10^{-3}	–	–	–

determined in order to obtain information about the three-dimensional structure of the molecule in solution. As shown in *Fig. 11,a*, three amide NH groups are almost unaffected by an increase of the concentration of (D_6)DMSO in the range of 0 to 12% (*v*/*v*). Based on the similarity with the results obtained for other described molecules, we assume that these are the NH H-atoms of Aib(3), Aib(5), and Aib(7), which are able to form three $1\leftarrow4$ intramolecular H-bonds. On the other hand, NH of Aib(1) shows a small but significant dependence on the (D_6)DMSO concentration. The experimental values of the temperature dependent NH resonances are shown in *Fig. 11,b*, and the values $\Delta\delta/\Delta T$ in the range of 265–314 K are compiled in *Table 4*. Only NH of Aib(1) shows a significant dependence on the temperature. The coefficient has been determined to be -10.2×10^{-3} ppm/K, which established that this NH H-atom is exposed to the solvent.

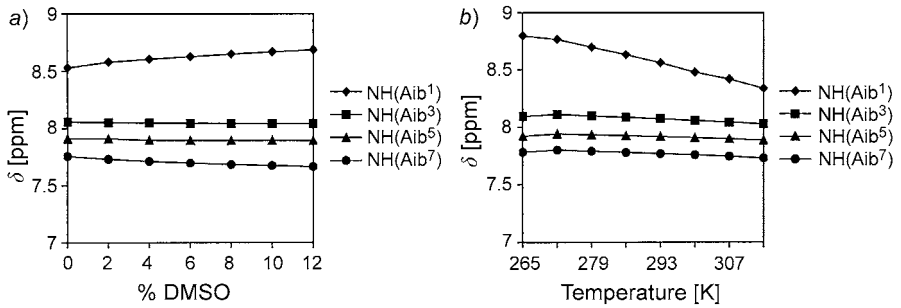

Fig. 11. *Chemical shifts of the NH resonances of* **13** *as a function* a) *of the* (D_6)*DMSO concentration* (in % *v*/*v*) *in* $CDCl_3$ *and* b) *of the temperature in the range of 265–314 K*

2.3.3. *Hexapeptide Ester* p-*BrBz-(Aib-Pro)*$_3$*-OMe* (**11**). The crystal structure and packing of **11** are shown in *Figs. 2* and *3*, respectively. In *Table 5*, the most relevant torsion angles of the peptide backbone are collected. The molecule also adopts a β-bend ribbon structure, which is stabilized by two $1\leftarrow4$ intramolecular H-bonds between the NH groups of the Aib(3) and Aib(5) residues, and the C=O groups of the *p*-BrBz-moiety and Pro(2), respectively (*Table 6*). In analogy to **15**, both C(γ)-*endo* (Pro(4)) and C(γ)-*exo* pyrrolidine ring puckerings (Pro(2) and Pro(6)) are observed.

The involvement of the NH groups of **11** in intramolecular H-bonds in solution was evaluated on the basis of the temperature dependence of the NH chemical shifts in the

Table 5. *Selected Main-Chain Torsion Angles* [°] *of* **11**

Angle	Aib(1)	Pro(2)	Aib(3)	Pro(4)	Aib(5)	Pro(6)
ϕ	– 53.8(7)	– 69.4(7)	– 53.4(7)	– 81.2(6)	– 56.9(7)	– 65.5(7)
ψ	– 28.9(7)	– 18.9(7)	– 46.8(7)	– 8.8(8)	– 45.8(7)	– 40.5(9)
ω	– 177.8(5)	178.6(5)	– 171.2(5)	– 177.8(5)	– 169.7(5)	– 174.4(5)

Table 6. *Intra- and Intermolecular H-Bonds in* **11**

D–H ··· A[a])	D–H [Å]	H ··· A [Å]	D ··· A [Å]	D–H ··· A [°]
N(1)–H(1) ··· O(12′)	0.88	2.22	3.044(6)	155
N(7)–H(7) ··· O(21)	0.88	2.04	2.901(6)	167
N(13)–H(13) ··· O(5)	0.88	2.18	2.978(6)	150

[a]) Primed atoms refer to the molecule in the symmetry-related position $1 - x, y, - z$.

temperature range of 265 – 314 K (*Fig. 12*). The temperature coefficients of the amide NH resonances are collected in *Table 4*. The value for the NH group of Aib(1) is $- 10.55 \times 10^{-3}$ ppm/K, which indicates that this H-atom is more or less freely exposed to the solvent. On the other hand, NH(Aib(3)) and NH(Aib(5)) show temperature dependences, which are *ca.* 10 times smaller. Therefore, it can be concluded that they form intramolecular H-bonds.

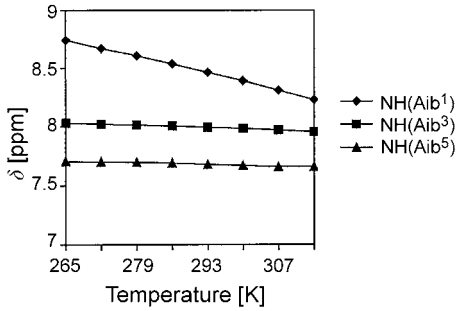

Fig. 12. *Chemical shifts of the NH resonances of* **11** *as a function of the temperature in the range of 265 – 314 K*

2.3.4. *Tetrapeptide Amide* p-*BrBz-(Aib-Pro)*$_2$-*NHC*$_6$*H*$_{13}$ (**14**). The crystal structure and packing of **14** are depicted in *Figs. 4* and *5*. As expected, the molecule adopts a β-bend ribbon structure, similar to the hexapeptide ester **11** (for relevant torsion angles, see *Table 7*). There is evidence for two $1 \leftarrow 4$ intramolecular H-bonds between the NH groups of the hexylamine residue and of Aib(3) and the C=O groups of the *p*-BrBz moiety and Pro(2), respectively (*Table 8*). Again, both types of pyrrolidine conformations are present (Pro(2): C(γ)-*exo*; Pro(4): C(γ)-*endo*).

Analogous ^{1}H-NMR experiments as in the previous cases were conducted in order to establish the H-bonding interactions and, on this basis, to propose the preferred

Table 7. *Selected Main-Chain Torsion Angles* [°] *of* **14**

Angle	Aib(1)	Pro(2)	Aib(3)	Pro(4)
ϕ	−48.1(3)	−63.7(2)	−55.9(3)	−81.1(2)
ψ	−38.7(3)	−28.5(3)	−48.9(2)	−4.4(3)
ω	179.7(2)	−178.0(2)	−166.7(2)	179.2(2)

Table 8. *Intra- and Intermolecular H-Bonds in* **14**

D–H···A[a])	D–H [Å]	H···A [Å]	D···A [Å]	D–H···A [°]
N(1)–H(1)···O(7)	0.83(2)	2.17(2)	2.956(3)	158(2)
N(6)–H(6)···O(13)	0.83(2)	2.12(2)	2.912(2)	160(2)
N(12)–H(12)···O(1′)	0.89(2)	1.96(2)	2.839(2)	170(2)

[a]) Primed atoms refer to the molecule in the symmetry-related position $1½ - x, 1 - y, -½ + z$.

conformation of **14** in solution. The results obtained from the solvent-titration experiment are presented in *Fig. 13*, *a*. It is obvious that two NH resonances are almost unaffected by the polarity of the solvent; we suggest that these correspond to the NH groups of Aib(3) and the hexylamine moiety, which form two intramolecular H-bonds, as in the crystalline state. In contrast, the NH H-atom resonance of Aib(1) shows a significant solvent dependence. The experimentally obtained $\Delta\delta/\Delta T$ values in the temperature range of 265–314 K are collected in *Table 4* (*Fig. 13*, *b*). The temperature coefficient for NH of Aib(1) is -10.58×10^{-3} ppm/K, which indicates that this NH H-atom is exposed to the solvent. The corresponding values for NH(Aib(3)) and NHC_6H_{13} are -2.8×10^{-3} and -2.73×10^{-3} ppm/K, respectively, providing a strong evidence that these NH groups are involved in intramolecular H-bonds.

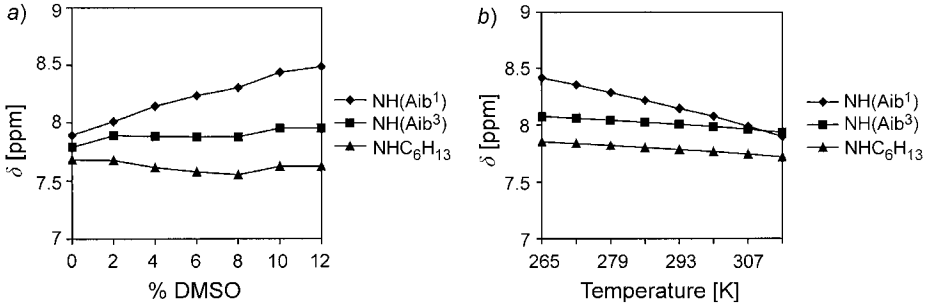

Fig. 13. *Chemical shifts of the NH resonances of* **14** *as a function* a) *of the (D₆)DMSO concentration* (in % *v/v*) *in* $CDCl_3$ *and* b) *of the temperature in the range of 265–314 K*

2.3.5. *Tetrapeptide Ester* p-*MeOBz-(Aib-Pro)₂-OMe* (**18**). The crystal structure and packing of **18** are shown in *Figs. 8* and *9*, respectively. The molecule adopts a helical conformation (β-turn; *Table 9*) with one $1 \leftarrow 4$ intramolecular H-bond between the NH group of the Aib(3) residue and the C=O group of the *p*-MeOBz-moiety (*Table 10*).

Table 9. *Selected Main-Chain Torsion Angles* [°] *of* **18**

Angle	Aib(1)	Pro(2)	Aib(3)	Pro(4)
ϕ	– 54.2(5)	– 74.7(5)	53.6(5)	– 66.8(5)
ψ	– 41.3(5)	– 15.9(6)	44.5(5)	– 38.6(7)
ω	– 169.7(4)	– 177.1(3)	169.4(4)	177.4(4)

Table 10. *Intra- and Intermolecular H-Bons in* **18**

D–H ··· A[a])	D–H [Å]	H ··· A [Å]	D ··· A [Å]	D–H ··· A [°]
N(1)–H(1) ··· O(9′)	0.94(5)	2.04(5)	2.908(5)	154(4)
N(6)–H(6) ··· O(15)	0.86(3)	2.11(4)	2.963(5)	169(4)

[a]) Primed atoms refer to the molecule in the symmetry-related position $x, y, 1+z$.

Table 11. *Pro Side-Chain Torsion Angles* [°] *of the Two Conformers of* **18**

Angle	Pro(2) conform. A	Pro(4) conform. A[a])	Pro(2) conform. B
θ	– 9.3(5)	– 4.6(6)	– 9.3(5)
χ^1	– 12.3(9)	26.1(6)	27.0(7)
χ^2	28.2(12)	– 38.2(7)	– 34.1(8)
χ^3	– 32.9(11)	34.5(7)	28.0(8)
χ^4	27.1(9)	– 18.4(6)	– 11.2(7)
Type of puckering	C(γ)-*exo*	C(γ)-*endo*	C(γ)-*endo*

[a]) The disorder for Pro(4) could not be modelled satisfactorily. Therefore, the values for Pro(4) may be partly an average of the two conformers.

The central five-membered ring of the peptide molecule has a disordered envelope conformation, in which the envelope flap atom, C(26), flips to either side of the ring, and, therefore, both C(γ)-*endo* and C(γ)-*exo* types of puckerings are found (*Table 11*).

As in all other cases, the preferred conformation of the tetrapeptide **18** in solution was established by ^{1}H-NMR experiments. The results obtained from the solvent-titration experiment are presented in *Fig. 14,a*. One NH resonance is almost unaffected when the concentration of (D_6)DMSO was increased from 0 to 12%, and it is very likely that this is the NH signal of Aib(3), which forms a $1 \leftarrow 4$ intramolecular H-bond as in the crystalline state. The chemical shift of the other NH group was strongly dependent on the (D_6)DMSO concentration. The experimentally obtained coefficients $\Delta\delta/\Delta T$ in the temperature range of 265–314 K (*Fig. 14,b*) are collected in *Table 4*. The temperature coefficient of the NH H-atom of Aib(1) is -12.1×10^{-3} ppm/K, *i.e.*, this NH H-atom is exposed to the solvent. The second NH group, with a temperature coefficient of -3.89×10^{-3} ppm/K, is assumed to be involved in an intramolecular H-bond.

3. Conclusions. – The presented results show that methyl *N*-(2,2-dimethyl-2*H*-azirin-3-yl)-L-prolinate (**1b**) is a suitable building block for the incorporation of the

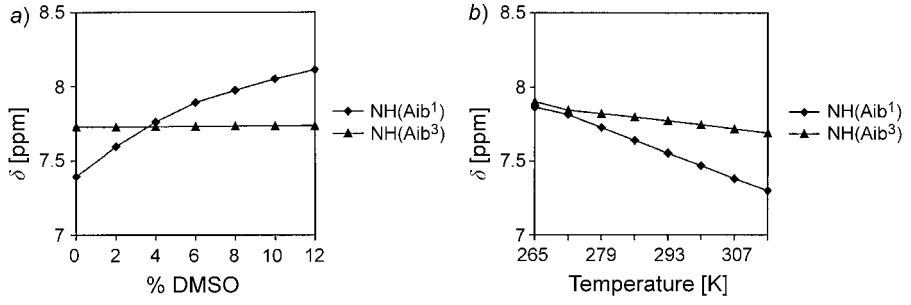

Fig. 14. *Chemical shifts of the NH resonances of* **18** *as a function* a) *of the (D6)DMSO concentration* (in % *v*/*v*) *in CDCl3 and* b) *of the temperature in the range of 265–314 K*

dipeptide unit Aib-Pro in a peptide backbone not only in the synthesis of segments of naturally occurring petaibols, such as zervamicin II-2 [8d], trichovirin I 1B [8e], and hypomurocin A1 [8f], but also in the cases of $(Aib\text{-}Pro)_n$ oligopeptides. Using the advantages of the 'azirine coupling', we prepared highly constrained peptides, containing consecutive (Aib-Pro) units, of the type *p*-BrBz-$(Aib\text{-}Pro)_n$-OMe, *p*-BrBz-$(Aib\text{-}Pro)_n$-NHC_6H_{13}, and *p*-MeO-$(Aib\text{-}Pro)_n$-OMe in order to study their conformations in the solid state and in solution. The results revealed that the preferred conformation is the β-bend ribbon structure, forming a sub-class of the 3_{10}-helices, in agreement with the results obtained by *Venkatachalapathi* and *Balaram* [5a] and *Toniolo* and co-workers [5c].

We thank the Analytical Sections of our institute for spectra and analyses, and the *Swiss National Science Foundation* and *F. Hoffmann-La Roche AG*, Basel, for financial support.

Experimental Part

1. *General.* Solvents were purified by standard procedures. TLC: *Merck* TLC aluminum sheets, silica gel *60* F_{254}. Column chromatography (CC): *Uetikon-Chemie*, silica gel *C-560* (0.04–0.063 mm, 230–400 mesh). M.p.: *Büchi Melting Point B-450* apparatus; uncorrected. IR Spectra: *Perkin-Elmer*, *Spectrum one FT-IR* spectrophotometer; in KBr unless otherwise stated; $\tilde{\nu}$ in cm^{-1}. NMR Spectra: *Bruker AC-300* (^1H, ^{13}C, DEPT) at 300 and 75 MHz, resp., or *Bruker DRX-600* (^1H, ^{13}C, HSQC, HMBC, COSY) at 600 and 150 MHz, resp., in $CDCl_3$ at 300 K unless otherwise stated; δ in ppm, coupling constants *J* in Hz; ^{13}C-signal multiplicities from DEPT spectra. MS: *Finnigan SSQ-700* (CI with NH_3), or *Finningan TSQ-700* instrument (ESI); *m*/*z* (rel. %).

2. *General Procedures. General Procedure 1* (*GP 1*). To a soln. of a peptide acid, 4-bromobenzoic acid (*p*-BrBz-OH) or 4-methoxybenzoic acid (*p*-MeOBz-OH) in dry THF or dry CH_2Cl_2, 2*H*-azirin-3-amine **1b** (1.1 mol-equiv.) was added, and the mixture was stirred at r.t. After completion of the reaction (TLC), the soln. was concentrated *in vacuo*, and the residue was purified by CC (SiO_2). The solvent was evaporated, and the solid material was used without further purification.

General Procedure 2 (*GP 2*). To a soln. of the corresponding peptide methyl ester in THF/MeOH/H_2O 3:1:1, $LiOH \cdot H_2O$ (4 mol-equiv.) was added. The mixture was stirred at r.t. After completion of the reaction (TLC), 1M HCl was added until pH 1 was reached, and the org. solvent was evaporated. The residue was extracted with CH_2Cl_2 or AcOEt, the org. phases were dried ($MgSO_4$), the solvent was evaporated, and the residue was dried under h.v.

General Procedure 3 (*GP 3*). To a soln. of the peptide acid in dry CH_2Cl_2 were added 1-hydroxy-1*H*-benzotriazole (HOBt, 1 mol-equiv.), 2-[(1*H*-benzotriazol-1-yl)oxy]-1,1,3,3-tetramethyluronium tetra-

fluoroborate (TBTU, 1 mol-equiv.), and (ethyl)(diisopropyl)amine (EtN(i-Pr)$_2$, DIEA; 2 mol-equiv.). A soln. of the amino component (1 mol-equiv.) was added dropwise, and the mixture was stirred at r.t. After completion of the reaction (TLC), the soln. was washed with 1M HCl, sat. $NaHCO_3$, and NaCl soln., dried ($MgSO_4$), evaporated, and purified by CC (SiO_2). The solvent was evaporated, and the solid material was used without further purification.

3. *Starting Materials.* The dipeptide synthon, *methyl 1-(2,2-dimethyl-2*H*-azirin-3-yl)-*L*-prolinate* (**1b**), was prepared according to [8b], all other chemicals were commercially available (*Fluka*, *Aldrich*).

4. *Synthesis of Aib-Pro Oligopeptides. Methyl* N*-(4-Bromobenzoyl)-2-methylalanylprolinate* (p*-BrBz-Aib-Pro-OMe*; **7**). According to *GP 1*, *p*-BrBz-OH (253 mg, 1.26 mmol) in dry THF (10 ml) and **1b** (272 mg, 1.386 mmol); stirring for 103 h; CC (CH_2Cl_2/MeOH from 150:1 to 20:1): 446 mg (89%) of **7**. Colorless crystals. M.p. 230°. IR: 3296*m*, 3054*m*, 2982*m*, 2952*m*, 2869*w*, 1750*s*, 1663*s*, 1616*s*, 1590*w*, 1538*s*, 1482*m*, 1422*s*, 1383*w*, 1362*m*, 1313*m*, 1286*w*, 1205*s*, 1168*s*, 1153*w*, 1096*w*, 1069*m*, 1012*m*, 989*w*, 906*m*, 847*m*, 792*w*, 764*m*, 749*w*, 709*w*, 655*w*. ^{1}H-NMR: 7.72 (br. *s*, NH); 7.70–7.64 (*m*, 2 arom. H); 7.75–7.50 (*m*, 2 arom. H); 4.61–4.57 (*m*, CH(α)(Pro)); 3.84–3.77 (*m*, 1 H of CH$_2$(δ)(Pro)); 3.73 (*s*, MeO); 3.67–3.59 (*m*, 1 H of CH$_2$(δ)(Pro)); 2.19–2.01 (*m*, CH$_2$(β)(Pro)); 2.03–1.90 (*m*, CH$_2$(γ)(Pro)); 1.79, 1.77 (2*s*, 2 Me(Aib)). ^{13}C-NMR: 172.8, 172.7 (2*s*, 2 C=O); 164.5 (*s*, Ar*C*=O); 133.8 (*s*, 1 arom. C); 131.7 (*d*, 2 arom. CH); 128.5 (*d*, 2 arom. CH); 126.0 (*s*, 1 arom. C); 61.1 (*d*, CH(α)(Pro)); 57.4 (*s*, C(α)(Aib)); 52.2 (*q*, MeO); 48.3 (*t*, CH$_2$(δ))(Pro)); 27.7 (*t*, CH$_2$(β)(Pro)); 25.8 (*t*, CH$_2$(γ)(Pro)); 23.0, 22.8 (2*q*, 2 Me(Aib)). CI-MS: 528 (100, [*M*(^{81}Br) + (Pro-OMe) + H]$^+$), 526 (90, [*M*(^{79}Br) + (Pro-OMe) + H]$^+$), 448 (18), 399 (9, [*M*(^{81}Br) + H]$^+$), 397 (9, [*M*(^{79}Br) + H]$^+$), 130 (52, [(Pro-OMe) + H]$^+$).

N-*[*N*-(4-Bromobenzoyl)-2-methylalanyl]proline* (p*-BrBz-Aib-Pro-OH*; **8**). According to *GP 2*, **7** (400 mg, 1.01 mmol) in 15 ml of THF/MeOH/H_2O, LiOH · H_2O (169.5 mg, 4.04 mmol); stirring for 3 h: 371 mg (96%) of **8**. The product was pure enough to be used in the next step without further purification. IR: 3281*m*, 3068*w*, 2988*m*, 2927*w*, 1714*s*, 1640*s*, 1622*s*, 1590*w*, 1531*m*, 1482*m*, 1470*w*, 1416*m*, 1383*w*, 1365*w*, 1323*m*, 1240*w*, 1205*s*, 1165*m*, 1111*w*, 1095*w*, 1071*m*, 1011*m*, 907*m*, 881*w*, 845*m*, 793*w*, 759*m*, 709*w*, 683*w*, 625*w*. ^{1}H-NMR ((D$_6$)DMSO): 8.59 (*s*, NH); 7.84–7.81 (*m*, 2 arom. H); 7.69–7.66 (*m*, 2 arom. H); 4.24–4.21 (*m*, CH(α)(Pro)); 3.70–3.66 (*m*, 1 H of CH$_2$(δ)(Pro)); 3.23–3.17 (*m*, 1 H of CH$_2$(δ)(Pro)); 1.94–1.86 (*m*, CH$_2$(β)(Pro)); 1.85–1.71 (*m*, CH$_2$(γ)(Pro)); 1.40 (*s*, 2 Me(Aib)). ^{13}C-NMR ((D$_6$)DMSO): 174.1, 171.5 (2*s*, 2 C=O); 164.9 (*s*, Ar*C*=O); 133.5 (*s*, 1 arom. C); 131.7 (*d*, 2 arom. CH); 130.1 (*d*, 2 arom. CH); 125.5 (*s*, 1 arom. C); 60.6 (*d*, CH(α)(Pro)); 56.7 (*s*, C(α)(Aib)); 47.8 (*t*, CH$_2$(δ))(Pro)); 27.9 (*t*, CH$_2$(β)(Pro)); 25.8 (*t*, CH$_2$(γ)(Pro)); 25.7, 24.9 (2*q*, 2 Me(Aib)). ESI-MS: 500 (96, [*M*(^{81}Br) + (Pro-OH) + H]$^+$), 498 (100, [*M*(^{79}Br) + (Pro-OH) + H]$^+$), 385 (50, [*M*(^{81}Br) + H]$^+$), 383 (54, [*M*(^{79}Br) + H]$^+$), 116 (100, [(Pro-OH) + H]$^+$).

N-*(*N*-{*N*-[*N*-(4-Bromobenzoyl)-2-methylalanyl]prolyl}-2-methylalanyl)proline Methyl Ester* (p*-BrBz-(Aib-Pro)$_2$-OMe*; **9**). According to *GP 1*, **8** (371 mg, 0.969 mmol) in dry CH_2Cl_2 (20 ml) and **1b** (209 mg, 1.066 mmol); stirring for 27 h, CC (CH_2Cl_2/MeOH from 150:1 to 20:1): 556 mg (99%) of **9**. M.p. 267° (dec.). IR: 3300*m*, 2984*m*, 2927*m*, 2874*m*, 1746*s*, 1646*s*, 1589*w*, 1537*s*, 1482*w*, 1468*w* 1403*m*, 1378*w*, 1326*w*, 1302*m*, 1243*w*, 1201*w*, 1168*s*, 1111*w*, 1094*m*, 1071*m*, 1049*w*, 956*w*, 944*w*, 907*w*, 880*w*, 848*s*, 761*s*, 708*w*, 631*w*, 625*m*, 612*w*. ^{1}H-NMR: 7.81–7.78 (*m*, 2 arom. H); 7.79 (*s*, NH); 7.64–7.61 (*m*, 2 arom. H, NH); 4.60–4.55 (*m*, CH(α)(Pro)); 4.40–4.36 (*m*, CH(α)(Pro)); 3.93–3.86 (*m*, 1 H of CH$_2$(δ)(Pro)); 3.76–3.71 (*m*, 1 H of CH$_2$(δ)(Pro)); 3.63 (*s*, MeO); 3.60–3.55 (*m*, 1 H of CH$_2$(δ)(Pro)); 3.26–3.23 (*m*, 1 H of CH$_2$(δ)(Pro)); 2.15–2.12 (*m*, 1 H of CH$_2$(β)(Pro)); 2.10–1.91 (*m*, 3 H of 2 CH$_2$(β)(Pro)); 1.84–1.78 (*m*, 4 H, 2 CH$_2$(γ)(Pro)); 1.66, 1.58, 1.54 (3*s*, 4 Me(Aib)). ^{13}C-NMR: 173.2, 172.4, 172.3, 171.3 (4*s*, 4 C=O); 165.8 (*s*, Ar*C*=O); 133.8 (*s*, 1 arom. C); 132.0 (*d*, 2 arom. CH); 129.1 (*d*, 2 arom. CH); 126.8 (*s*, 1 arom. C); 62.7, 60.6 (2*d*, 2 CH(α)(Pro)); 57.5, 56.6 (2*s*, 2 C(α)(Aib)); 51.9 (*q*, MeO); 48.2, 47.7 (2*t*, 2 CH$_2$(δ))(Pro)); 28.4, 28.0 (2*t*, 2 CH$_2$(β)(Pro)); 26.0, 25.9 (2*t*, 2 CH$_2$(γ)(Pro)); 25.9, 25.1, 24.7, 24.5 (4*q*, 4 Me(Aib)). ESI-MS: 603 (18, [*M*(^{81}Br) + Na]$^+$), 601 (19, [*M*(^{79}Br) + Na]$^+$), 581 (10, [*M*(^{81}Br) + H]$^+$), 579 (10, [*M*(^{79}Br) + H]$^+$), 452 (100, [*M*(^{81}Br) – (Pro-OMe) + H]$^+$), 450 (92, [*M*(^{79}Br) – (Pro-OMe) + H]$^+$), 367 (9, [*M*(^{81}Br) – (Aib-Pro-OMe) + H]$^+$), 365 (10, [*M*(^{79}Br) – (Aib-Pro-OMe) + H]$^+$).

N-*(*N*-{*N*-[*N*-(4-Bromobenzoyl)-2-methylalanyl]prolyl}-2-methylalanyl)proline* (p*-BrBz-(Aib-Pro)$_2$-OH*; **10**). According to *GP 2*, **9** (503 mg, 0.869 mmol) in 20 ml of THF/MeOH/H_2O, LiOH · H_2O (145.8 mg, 3.476 mmol); stirring for 22 h: 455 mg (93%) of **10**. The isolated peptide acid was pure enough to be used in the next step without further purification. ^{1}H-NMR (CD_3OD): 8.72, 8.04 (2*s*, 2 NH); 7.83–

7.79 (*m*, 2 arom. H); 7.69–7.64 (*m*, 2 arom. H); 4.51–4.46 (*m*, CH(*α*)(Pro)); 4.44–4.40 (*m*, CH(*α*)(Pro)); 3.82–3.74 (*m*, 1 H of CH_2(*δ*)(Pro)); 3.72–3.68 (*m*, 2 H of 2 CH_2(*δ*)(Pro)); 3.42–3.34 (*m*, 1 H of CH_2(*δ*)(Pro)); 2.22–2.05 (*m*, 2 H of 2 CH_2(*β*)(Pro)); 1.98–1.75 (*m*, 6 H, CH_2(*β*)(Pro), 2 CH_2(*γ*)(Pro)); 1.59, 1.56, 1.54, 1.50 (4*s*, 4 Me(Aib)). ^{13}C-NMR (CD_3OD): 173.8, 171.6, 171.2, 171.1 (4*s*, 4 C=O); 165.5 (*s*, Ar*C*=O); 132.7 (*s*, 1 arom. C); 131.6 (*d*, 2 arom. CH); 129.8 (*d*, 2 arom. CH); 125.7 (*s*, 1 arom. C); 61.8, 60.2 (2*d*, 2 CH(*α*)(Pro)); 56.7, 55.7 (2*s*, 2 C(*α*)(Aib)); 47.9, 47.1 (2*t*, 2 CH_2(*δ*))(Pro)); 28.2, 27.7 (2*t*, 2 CH_2(*β*)(Pro)); 25.5, 25.4 (2*t*, 2 CH_2(*γ*)(Pro)); 25.8, 25.5, 25.2, 24.5 (4*q*, 4 Me(Aib)). ESI-MS: 589 (32, $[M(^{81}Br)+Na]^+$), 587 (29, $[M(^{79}Br)+Na]^+$), 567 (13, $[M(^{81}Br)+H]^+$), 565 (13, $[M(^{79}Br)+H]^+$), 452 (100, $[M(^{81}Br)-(Pro\text{-}OH)+H]^+$), 450 (98, $[M(^{79}Br)-(Pro\text{-}OH)+H]^+$), 367 (18, $[M(^{81}Br)-(Aib\text{-}Pro\text{-}OH)+H]^+$), 365 (18, $[M(^{79}Br)-(Aib\text{-}Pro\text{-}OH)+H]^+$).

N-*{*N-*[*N-*(*N-*{*N-*[*-N-*(4-Bromobenzoyl)-2-methylalanyl]prolyl}-2-methylalanyl)prolyl]-2-methyl}-alanyl}proline Methyl Ester* (p-*BrBz-(Aib-Pro)$_3$-OMe*; **11**). According to *GP 1*, **10** (455 mg, 0.805 mmol) in dry CH_2Cl_2 (20 ml) and **1b** (174 mg, 0.886 mmol); stirring for 96 h, CC (CH_2Cl_2/MeOH from 150:1 to 20:1): 553 mg (90%) of **11**. M.p. 302° (dec.). IR: 3272*m*, 2981*m*, 2945*m*, 2880*w*, 1749*s*, 1640*s*, 1588*w*, 1536*s*, 1480*w*, 1470*w*, 1406*s*, 1363*w*, 1198*m*, 1168*s*, 1110*w*, 1096*w*, 1071*w*, 1047*w*, 1009*m*, 853*m*, 810*w*, 760*m*, 709*w*, 664*w*, 611*m*. ^{1}H-NMR: 8.32, 7.98 (2*s*, 2 NH); 7.87–7.84 (*m*, 2 arom. H); 7.67–7.63 (*m*, 2 arom. H, NH); 7.66 (*s*, NH); 4.59–4.54 (*m*, 2 CH(*α*)(Pro)); 4.38–4.34 (*m*, CH(*α*)(Pro)); 4.00–3.86 (*m*, 2 H of 3 CH_2(*δ*)(Pro)); 3.83–3.76 (*m*, 2 H of 3 CH_2(*δ*)(Pro)); 3.61 (*s*, MeO); 3.27–3.18 (*m*, 2 H of 3 CH_2(*δ*)(Pro)); 2.27–2.07 (*m*, 4 H); 2.04–1.77 (*m*, 8 H); 1.64, 1.61, 1.59, 1.54, 1.49, 1.48 (6*s*, 6 Me(Aib)). ^{13}C-NMR: 173.4, 172.8, 172.7, 172.7, 172.2, 171.9 (6*s*, 6 C=O); 166.3 (*s*, Ar*C*=O); 132.1 (*d*, 2 arom. CH); 131.9 (*s*, 1 arom. C); 129.3 (*d*, 2 arom. CH); 126.9 (*s*, 1 arom. C); 62.5, 62.3, 60.6 (3*d*, 3 CH(*α*)(Pro)); 57.5, 56.5, 56.4 (3*s*, 3 C(*α*)(Aib)); 51.8 (*q*, MeO); 48.4, 48.1, 47.8 (3*t*, 3 CH_2(*δ*))(Pro)); 29.0, 28.2, 28.1 (3*t*, 3 CH_2(*β*)(Pro)); 26.3, 26.1, 25.9 (3*t*, 3 CH_2(*γ*)(Pro)); 25.9, 25.1, 24.5, 24.4, 24.4, 24.1 (6*q*, 6 Me(Aib)). ESI-MS: 785 (100, $[M(^{81}Br)+Na]^+$), 783 (90, $[M(^{79}Br)+Na]^+$), 634 (7, $[M(^{81}Br)-(Pro\text{-}OMe)+H]^+$), 632 (7, $[M(^{79}Br)-(Pro\text{-}OMe)+H]^+$).

Suitable crystals of **11** for the X-ray crystal-structure determination were grown from CH_2Cl_2/AcOEt by slow evaporation of the solvent at r.t.

*1-[*N-*(4-Bromobenzoyl)-2-methylalanyl]-*N-*{1-[2-(hexylcarbamoyl)pyrrolidin-2-yl]-2-methyl-1-oxopropan-2-yl}prolinamide* (p-*BrBz-(Aib-Pro)$_2$-NHC$_6$H$_{13}$*; **14**). According to *GP 3*, **10** (281 mg, 0.497 mmol), hexylamine (60.35 mg, 0.596 mmol), HOBt (67.2 mg, 0.497 mmol), TBTU (159.6 mg, 0.497 mmol), DIEA (128.5 mg, 0.994 mmol), dry CH_2Cl_2 (15 ml); stirring for 20 h, CC (CH_2Cl_2/MeOH from 150:1 to 20:1): 290 mg (90%) of **14**. M.p. 132°. IR: 3284*m*, 2983*w*, 2931*m*, 2872*w*, 1639*s*, 1589*w*, 1542*s*, 1483*w*, 1468*w* 1403*m*, 1378*w*, 1363*w*, 1316*w*, 1200*w*, 1174*w*, 1170*m*, 1010*w*, 922*w*, 851*m*, 761*m*, 728*m*. ^{1}H-NMR: 8.03, 7.99 (2*s*, 2 NH); 7.87–7.84 (*m*, 2 arom. H); 7.75 (*s*, NH); 7.63–7.60 (*m*, 2 arom. H); 4.62–4.57 (*m*, CH(*α*)(Pro)); 4.55–4.51 (*m*, CH(*α*)(Pro)); 3.96–3.85 (*m*, 2 H of 2 CH_2(*δ*)(Pro)); 3.79–3.65 (*m*, 1 H of 2 CH_2(*δ*)(Pro)); 3.35–3.12 (*m*, 2 H); 3.06–2.96 (*m*, 1 H of 2 CH_2(*δ*)(Pro)); 2.33–2.11 (*m*, 2 H); 2.02–1.81 (*m*, 6 H); 1.76–1.51 (*m*, 8 H); 1.49, 1.43 (2*s*, 4 Me(Aib)); 0.88–0.84 (*m*, 3 H). ^{13}C-NMR: 172.6, 172.6, 172.4, 172.3 (4*s*, 4 C=O); 166.3 (*s*, Ar*C*=O); 131.9 (*d*, 2 arom. CH); 131.8 (*s*, 1 arom. C); 129.2 (*d*, 2 arom. CH); 126.9 (*s*, 1 arom. C); 62.4 (*d*, CH(*α*)(Pro)); 57.4, 56.5 (2*s*, 2 C(*α*)(Aib)); 54.9 (*d*, CH(*α*)(Pro)); 48.3, 48.2 (2*t*, 2 CH_2(*δ*))(Pro)); 39.6 (*t*, CH_2); 31.5, 29.2, 28.9, 28.8, 28.8, 26.6, 26.2, 25.8 (8*t*, 8 CH_2); 26.4, 26.3, 24.4, 24.1 (4*q*, 4 Me(Aib)); 14.1 (*q*, Me). ESI-MS: 672 (15, $[M(^{81}Br)+Na]^+$), 670 (15, $[M(^{79}Br)+Na]^+$), 650 (27, $[M(^{81}Br)+H]^+$), 648 (24, $[M(^{79}Br)+H]^+$) 452 (28, $[M(^{81}Br)-(Pro\text{-}NHC_6H_{13})+H]^+$), 450 (28, $[M(^{79}Br)-(Pro\text{-}NHC_6H_{13})+H]^+$), 199 (5, $[(Pro\text{-}NHC_6H_{13})+H]^+$), 130 (100, $[(Pro\text{-}OMe)+H]^+$).

Suitable crystals of **14** for the X-ray crystal-structure determination were grown from CH_2Cl_2 by slow evaporation of the solvent at r.t.

N-*{*N-*[*N-*(*N-*{*N-*[*N-*(4-Bromobenzoyl)-2-methylalanyl]prolyl}-2-methylalanyl)prolyl]-2-methylalanyl}proline* (p-*BrBz-(Aib-Pro)$_3$-OH*; **12**). According to *GP 2*, **11** (500 mg, 0.657 mmol) in 30 ml of THF/MeOH/H_2O, LiOH·H_2O (110 mg, 2.628 mmol), stirring for 24 h: 490 mg (99%) of **12**.The isolated peptide acid was pure enough to be used in the next step without further purification. ^{1}H-NMR ((D_6)DMSO): 12.1 (br. *s*, OH); 9.22 (*s*, NH); 7.98–7.94 (*m*, 2 arom. H); 7.93 (*s*, NH); 7.74–7.71 (*m*, 2 arom. H, NH); 7.59 (*s*, NH); 4.38–4.33 (*m*, 2 CH(*α*)(Pro)); 4.21–4.17 (*m*, CH(*α*)(Pro)); 3.78–3.59 (*m*, 3 H of 3 CH_2(*δ*)(Pro)); 3.59–3.55 (*m*, 2 H of 3 CH_2(*δ*)(Pro)); 3.18–3.14 (*m*, 1 H of 3 CH_2(*δ*)(Pro));

2.09–2.02 (*m*, 3 H); 1.87–1.63 (*m*, 9 H); 1.48, 1.45, 1.37, 1.30 (4*s*, 6 Me(Aib)). ^{13}C-NMR ((D$_6$)DMSO): 173.6, 172.7, 172.2, 172.0, 171.7, 171.1 (6*s*, 6 C=O); 165.6 (*s*, Ar*C*=O); 132.4 (*s*, 1 arom. C); 131.4 (*d*, 2 arom. CH); 129.9 (*d*, 2 arom. CH); 125.6 (*s*, 1 arom. C); 61.9, 61.3, 60.1 (3*d*, 3 CH(α)(Pro)); 56.6, 55.7, 55.5 (3*s*, 3 C(α)(Aib)); 47.9, 47.4, 47.1 (3*t*, 3 CH$_2$(δ))(Pro)); 28.4, 28.1, 27.6 (3*t*, 3 CH$_2$(β)(Pro)); 25.7, 25.2, 25.0 (3*t*, 3 CH$_2$(γ)(Pro)); 25.7, 25.2, 24.9, 24.3, 24.2, 23.9 (6*q*, 6 Me(Aib)). ESI-MS: 771 (34, [*M*(^{81}Br) + Na]$^+$), 769 (23, [*M*(^{79}Br) + Na]$^+$), 749 (17, [*M*(^{81}Br) + H]$^+$), 747 (17, [*M*(^{79}Br) + H]$^+$), 634 (100, [*M*(^{81}Br) – (Pro-OH) + H]$^+$), 632 (75, [*M*(^{79}Br) – (Pro-OH) + H]$^+$), 452 (20, [*M*(^{81}Br) – (Pro-Aib-Pro-OH) + H]$^+$), 450 (20, [*M*(^{79}Br) – (Pro-Aib-Pro-OH) + H]$^+$).

N-*[*N-*(*N-*{*N-*[*N-*(*N-*{*N-*[*N-*(4-Bromobenzoyl)-2-methylalanyl]prolyl}-2-methylalanyl)prolyl]-2-methylalanyl}prolyl)-2-methylalanyl]proline Methyl Ester* (p-*BrBz-(Aib-Pro)$_4$-OMe*; **13**). According to *GP 1*, **12** (490 mg, 0.656 mmol) in dry THF (30 ml) and **1b** (141 mg, 0.72 mmol); stirring for 120 h, CC (CH$_2$Cl$_2$/MeOH from 150:1 to 10:1): 151 mg (24%) of **13**. M.p. 302° (dec.). IR: 3285*m*, 2984*m*, 2938*m*, 2876*w*, 1745*m*, 1643*s*, 1590*w*, 1536*m*, 1469*w*, 1407*s*, 1380*w*, 1363*w*, 1304*w*, 1245*w*, 1202*m*, 1171*m*, 1094*w*, 1071*w*, 1011*m*, 926*w*, 849*w*, 761*m*, 615*w*. ^{1}H-NMR ((D$_6$)DMSO): 8.98, 7.95 (2*s*, 2 NH); 7.90–7.87 (*m*, 2 arom. H); 7.81 (*s*, NH); 7.76–7.73 (*m*, 2 arom. H); 7.57 (*s*, NH); 4.41–4.31 (*m*, 3 CH(α)(Pro)); 4.25–4.21 (*m*, CH(α)(Pro)); 3.78–3.61 (*m*, 6 H of 4 CH$_2$(δ)(Pro)); 3.59 (*s*, MeO); 3.57–3.51 (*m*, 1 H of CH$_2$(δ)(Pro)); 3.19–3.16 (*m*, 1 H of CH$_2$(δ)(Pro)); 2.13–1.99 (*m*, 4 H); 1.97–1.63 (*m*, 12 H); 1.48, 1.47, 1.38, 1.36, 1.30 (5*s*, 8 Me(Aib)). ^{13}C-NMR ((D$_6$)DMSO): 173.2, 172.7, 172.5, 172.1, 172.0, 171.8, 171.5, 171.4 (8*s*, 8 C=O); 166.0 (*s*, Ar*C*=O); 132.9 (*s*, 1 arom. C); 131.6 (*d*, 2 arom. CH); 130.1 (*d*, 2 arom. CH); 126.0 (*s*, 1 arom. C); 62.3, 61.9, 61.7, 60.3 (4*d*, 4 CH(α)(Pro)); 56.9, 56.2, 56.0, 55.8 (4*s*, 4 C(α)(Aib)); 51.8 (*q*, MeO); 48.3, 47.9, 47.6, 47.5 (4*t*, 4 CH$_2$(δ))(Pro)); 28.9, 28.8, 28.5, 27.9 (4*t*, 4 CH$_2$(β)(Pro)); 25.6, 25.4, 25.3, 25.2 (4*t*, 4 CH$_2$(γ)(Pro)); 26.1, 26.0, 25.9, 25.4, 24.5, 24.4, 24.3, 24.2 (8*q*, 8 Me(Aib)). ESI-MS: 967 (68, [*M*(^{81}Br) + Na]$^+$), 965 (47, [*M*(^{79}Br) + Na]$^+$), 816 (100, [*M*(^{81}Br) – (Pro-OMe) + H]$^+$), 814 (89, [*M*(^{79}Br) – (Pro-OMe) + H]$^+$), 634 (76, [*M*(^{81}Br) – (Pro-Aib-Pro-OMe) + H]$^+$), 632 (83, [*M*(^{79}Br) – (Pro-Aib-Pro-OMe) + H]$^+$), 452 (26, [*M*(^{81}Br) – (Pro-Aib-Pro-Aib-Pro-OMe) + H]$^+$), 450 (25, [*M*(^{79}Br) – (Pro-Aib-Pro-Aib-Pro-OMe) + H]$^+$).

N-*[*N-*(*N-*{*N-*[*N-*(*N-*{*N-*[*N-*(4-Bromobenzoyl)-2-methylalanyl]prolyl}-2-methylalanyl)prolyl]-2-methylalanyl}prolyl)-2-methylalanyl]proline* (p-*BrBz-(Aib-Pro)$_4$-OH*). According to *GP 2*, **13** (120 mg, 0.127 mmol) in 18 ml of THF/MeOH/H$_2$O, LiOH · H$_2$O (21 mg, 0.508 mmol), stirring for 20 h: 118 mg (89%) of the tetrapeptide acid. The isolated product was pure enough to be used in the next step without further purification. ^{1}H-NMR: 8.23, 8.17, 8.05, 8.01 (4*s*, 4 NH); 7.85–7.84 (*m*, 2 arom. H); 7.65–7.62 (*m*, 2 arom. H); 4.59–4.56 (*m*, 4 CH(α)(Pro)); 4.00–3.88 (*m*, 2 H of 4 CH$_2$(δ)(Pro)); 3.85–3.67 (*m*, 5 H of 4 CH$_2$(δ)(Pro)); 3.30–3.18 (*m*, 1 H of CH$_2$(δ)(Pro)); 2.84–2.04 (*m*, 4 H); 1.92–1.85 (*m*, 12 H); 1.65, 1.62, 1.60, 1.55, 1.52, 1.47, 1.46, 1.41 (8*s*, 8 Me(Aib)). ^{13}C-NMR: 173.9, 173.8, 173.7, 172.9, 172.8, 172.8, 172.7, 172.5 (8*s*, 8 C=O); 166.4 (*s*, Ar*C*=O); 131.9 (*d*, 2 arom. CH); 131.7 (*s*, 1 arom. C); 129.1 (*d*, 2 arom. CH); 126.7 (*s*, 1 arom. C); 62.5, 62.2, 62.0, 61.9 (4*d*, 4 CH(α)(Pro)); 57.3, 56.4, 56.3, 56.3 (4*s*, 4 C(α)(Aib)); 48.5, 48.4, 48.2, 48.2 (4*t*, 4 CH$_2$(δ))(Pro)); 29.6, 29.3, 28.9, 28.5 (4*t*, 4 CH$_2$(β)(Pro)); 26.1, 25.8, 25.8, 25.8 (4*t*, 4 CH$_2$(γ)(Pro)); 30.7, 26.1, 26.1, 26.1, 24.2, 23.9, 23.6, 23.4 (8*q*, 8 Me(Aib)).

*1-[*N-*(*N-*[*N-*(*N-*{*N-*[*N-*(4-Bromobenzoyl)-2-methylalanyl]prolyl}-2-methylalanyl)prolyl]-2-methylalanyl}prolyl)-2-methylalanyl]-*N-*hexylprolinamide* (p-*BrBz-(Aib-Pro)$_4$-NHC$_6$H$_{13}$*; **15**). According to *GP 3*, the tetrapeptide acid (103 mg, 0.111 mmol), hexylamine (13.5 mg, 0.133 mmol), HOBt (15 mg, 0.111 mmol), TBTU (35.6 mg, 0.111 mmol), DIEA (28.7 mg, 0.222 mmol), dry CH$_2$Cl$_2$ (12 ml); stirring for 19 h; CC (CH$_2$Cl$_2$/MeOH from 150:1 to 10:1): 49.5 mg (44%) of **15**. M.p. 132°. IR: 3284*s*, 2983*m*, 2934*m*, 2873*m*, 1643*s*, 1590*w*, 1539*s*, 1469*m*, 1404*s*, 1378*w*, 1363*w*, 1306*m*, 1245*w*, 1201*m*, 1174*m*, 1146*w*, 1095*w*, 1071*w*, 1013*m*, 933*w*, 850*m*, 761*m*, 614*w*. ^{1}H-NMR: 8.49, 8.07, 8.03 (3*s*, 3 NH); 7.91–7.88 (*m*, 2 arom. H); 7.77 (*s*, NH); 7.65–7.62 (*m*, 2 arom. H, NH); 4.61–4.58 (*m*, 3 CH(α)(Pro)); 4.51–4.46 (*m*, CH(α)(Pro)); 4.01–3.96 (*m*, 2 H of 4 CH$_2$(δ)(Pro)); 3.93–3.77 (*m*, 5 H of 4 CH$_2$(δ)(Pro)); 3.29–3.21 (*m*, CH$_2$); 3.19–2.96 (*m*, 1 H, CH$_2$(δ)(Pro)); 2.24–2.15 (*m*, 4 H); 2.06–1.84 (*m*, 12 H); 1.81–1.73 (*m*, 8 H); 1.65, 1.63, 1.60, 1.56, 1.52, 1.51, 1.49, 1.47 (8*s*, 8 Me(Aib)); 0.88–0.84 (*m*, Me). ^{13}C-NMR: 172.8, 172.8, 172.7, 172.6, 172.5, 172.4, 172.3, 172.2 (8*s*, 8 C=O); 166.3 (*s*, Ar*C*=O); 131.9 (*d*, 2 arom. CH); 131.8 (*s*, 1 arom. C); 139.3 (*d*, 2 arom. CH); 126.8 (*s*, 1 arom. C); 62.5, 62.4, 62.3, 62.1 (4*d*, 4 CH(α)(Pro)); 57.5, 56.4, 53.8, 53.8 (4*s*, 4 C(α)(Aib)); 48.2, 48.1, 48.0, 47.9 (4*t*, 4 CH$_2$(δ))(Pro)); 39.4, 33.7, 31.5 (3*t*, 3 CH$_2$); 29.3, 29.2, 29.0, 28.9 (4*t*, 4 CH$_2$(β)(Pro)); 26.5 (*t*, CH$_2$); 26.1, 26.0, 25.9, 25.6 (4*t*, 4 CH$_2$(γ)(Pro)); 22.5 (*t*,

CH_2); 25.8, 25.7, 24.4, 24.3, 24.1, 24.0, 23.9, 23.8 (8*q*, 8 Me(Aib)); 14.0 (*q*, Me). ESI-MS: 1143 (5, $[M(^{81}Br) + (Pro\text{-}OMe) + H]^+$), 1141 (5, $[M(^{79}Br) + (Pro\text{-}OMe) + H]^+$), 1036 (10, $[M(^{81}Br) + Na]^+$), 1034 (10, $[M(^{79}Br) + Na]^+$), 816 (100, $[M(^{81}Br) - (Pro\text{-}NHC_6H_{13}) + H]^+$), 814 (96, $[M(^{79}Br) - (Pro\text{-}NHC_6H_{13}) + H]^+$), 634 (31, $[M(^{81}Br) - (Pro\text{-}Aib\text{-}Pro\text{-}NHC_6H_{13}) + H]^+$), 632 (29, $[M(^{79}Br) - (Pro\text{-}Aib\text{-}Pro\text{-}C_6H_{13}) + H]^+$), 452 (5, $[M(^{81}Br) - (Pro\text{-}Aib\text{-}Pro\text{-}Aib\text{-}Pro\text{-}NHC_6H_{13}) + H]^+$), 450 (5, $[M(^{79}Br) - (Pro\text{-}Aib\text{-}Pro\text{-}Aib\text{-}Pro\text{-}NHC_6H_{13}) + H^+$).

Suitable crystals of **15** for the X-ray crystal-structure determination were grown from CH_2Cl_2/AcOEt/hexane by slow evaporation of the solvent at r.t.

N-*[*N-*(4-Methoxybenzoyl)-2-methylalanyl]proline Methyl Ester* (p-*MeOBz-Aib-Pro-OMe*; **16**). According to *GP 1*, *p*-MeOBz-OH (109.6 mg, 0.72 mmol) in dry THF (15 ml) and **1b** (155.2 mg, 0.792 mmol); stirring for 42 h; CC (CH_2Cl_2/MeOH from 150 : 1 to 90 : 1): 214 mg (85%) of **16**. Colorless crystals. M.p. 165°. IR: 3326*m*, 2987*m*, 2954*m*, 2839*w*, 1748*s*, 1653*s*, 1616*s*, 1577*w*, 1536*s*, 1504*s*, 1418*s*, 1377*w*, 1358*m*, 1317*m*, 1295*w*, 1256*s*, 1176*s*, 1110*w*, 1030*m*, 946*w*, 905*m*, 847*m*, 798*w*, 772*m*, 746*w*, 648*w*. ^{1}H-NMR: 7.79–7.75 (*m*, 2 arom. H); 7.36 (*s*, NH); 6.93–6.88 (*m*, 2 arom. H); 4.62–4.59 (*m*, CH(α)(Pro)); 3.84 (*s*, *Me*OC_6H_4); 3.82–3.76 (*m*, 1 H of CH_2(δ)(Pro)); 3.74 (*s*, MeO(Pro)); 3.65–3.59 (*m*, 1 H of CH_2(δ)(Pro)); 2.17–2.11 (*m*, CH_2(β)(Pro)); 2.09–1.91 (*m*, CH_2(γ)(Pro)); 1.78, 1.75 (2*s*, 2 Me(Aib)). ^{13}C-NMR: 172.9, 172.8 (2*s*, 2 C=O); 165.2 (*s*, Ar*C*=O); 162.2 (*s*, 1 arom. C); 128.7 (*d*, 2 arom. CH); 127.1 (*s*, 1 arom. C); 113.7 (*d*, 2 arom. CH); 60.9 (*d*, CH(α)(Pro)); 57.1 (*s*, C(α)(Aib)); 55.4 (*q*, *Me*OC_6H_4); 52.1 (*q*, MeO(Pro)); 48.2 (*t*, CH_2(δ))(Pro)); 27.8 (*t*, CH_2(β)(Pro)); 25.8 (*t*, CH_2(γ)(Pro)); 23.6, 23.4 (2*q*, 2 Me(Aib)). ESI-MS: 478 (35, $[M + (Pro\text{-}OMe) + H]^+$), 349 (34, $[M + H]^+$), 220 (14, $[M - (Pro\text{-}OMe) + H]^+$), 130 (100, $[(Pro\text{-}OMe) + H]^+$). Anal. calc. for $C_{18}H_{24}N_2O_5$ (348.39): C 62.05, H 6.94, N 8.04; found: C 61.81, H 7.20, N 7.87.

N-*[*N-*(4-Methoxybenzoyl)-2-methylalanyl]proline* (p-*MeOBz-Aib-Pro-OH*; **17**). According to *GP 2*, **16** (100 mg, 0.287 mmol) in 15 ml of THF/MeOH/H_2O, LiOH·H_2O (48.2 mg, 1.148 mmol); stirring for 20 h: 94 mg (98%) of **17**. The product was pure enough to be used in the next step without further purification. M.p. 155°. ^{1}H-NMR: 7.82–7.79 (*m*, 2 arom. H); 7.13 (*s*, NH); 6.94–6.89 (*m*, 2 arom. H); 4.68–4.64 (*m*, CH(α)(Pro)); 3.84 (*s*, *Me*OC_6H_4); 3.68–3.62 (*m*, 1 H of CH_2(δ)(Pro)); 3.56–3.51 (*m*, 1 H of CH_2(δ)(Pro)); 2.14–1.85 (*m*, CH_2(β)(Pro), CH_2(γ)(Pro)); 1.68, 1.65 (2*s*, 2 Me(Aib)). ^{13}C-NMR: 173.9, 173.5 (2*s*, 2 C=O); 166.5 (*s*, Ar*C*=O); 162.7 (*s*, 1 arom. C); 129.1 (*d*, 2 arom. CH); 125.4 (*s*, 1 arom. C); 113.9 (*d*, 2 arom. CH); 61.7 (*d*, CH(α)(Pro)); 57.2 (*s*, C(α)(Aib)); 55.4 (*q*, *Me*OC_6H_4); 48.4 (*t*, CH_2(δ))(Pro)); 27.5 (*t*, CH_2(β)(Pro)); 25.9 (*t*, CH_2(γ)(Pro)); 25.2, 24.5 (2*q*, 2 Me(Aib)). ESI-MS: 450 (40, $[M + (Pro\text{-}OH) + H]^+$), 357 (30, $[M + Na]^+$), 335 (74, $[M + H]^+$), 220 (100, $[M - (Pro\text{-}OH) + H]^+$), 135 (26, $[M - (Aib\text{-}Pro\text{-}OH) + H]^+$), 116 (33, $[(Pro\text{-}OH) + H]^+$). Anal. calc. for $C_{17}H_{22}N_2O_5$ (334.37): C 61.07, H 6.63, N 8.38; found: C 60.22, H 6.89, N 7.85.

N-*(*N-*[*N-*(4-Methoxybenzoyl)-2-methylalanyl]prolyl}-2-methylalanyl)proline Methyl Ester* (p-*MeOBz-(Aib-Pro)$_2$-OMe*, **18**). According to *GP 1*, **17** (94 mg, 0.281 mmol) in dry CH_2Cl_2 (15 ml) and **1b** (61 mg, 0.3091 mmol); stirring for 48 h, CC (CH_2Cl_2/MeOH from 170 : 1 to 15 : 1): 115 mg (78%) of **18**. M.p. 132°. IR: 3384*m*, 2986*m*, 2949*m*, 2877*w*, 1749*s*, 1639*s*, 1573*w*, 1542*m*, 1504*m*, 1406*s*, 1363*m*, 1298*w*, 1257*m*, 1177*s*, 1093*w*, 1025*m*, 924*w*, 900*w*, 849*m*, 791*w*, 773*m*, 751*w*, 729*w*, 699*w*, 610*w*. ^{1}H-NMR: 7.85–7.83 (*m*, 2 arom. H); 7.67, 7.11 (2*s*, 2 NH); 6.99–6.95 (*m*, 2 arom. H); 4.67–4.62 (*m*, CH(α)(Pro)); 4.49–4.44 (*m*, CH(α)(Pro)); 3.87 (*s*, *Me*OC_6H_4); 3.84–3.70 (*m*, CH_2(δ)(Pro)); 3.68 (*s*, MeO(Pro)); 3.62–3.57 (*m*, 1 H of CH_2(δ)(Pro)); 3.31–3.25 (*m*, 1 H of CH_2(δ)(Pro)); 2.11–1.94 (*m*, 2 CH_2(β)(Pro)); 1.90–1.72 (*m*, 2 CH_2(γ)(Pro)); 1.66, 1.61, 1.57 (3*s*, 4 Me(Aib)). ^{13}C-NMR: 173.3, 172.3, 172.1, 171.0 (4*s*, 4 C=O); 166.0 (*s*, Ar*C*=O); 162.7 (*s*, 1 arom. C); 128.9 (*d*, 2 arom. CH); 125.2 (*s*, 1 arom. C); 113.9 (*d*, 2 arom. CH); 62.5, 60.5 (2*d*, 2 CH(α)(Pro)); 57.1, 56.6 (2*s*, 2 C(α)(Aib)); 55.4 (*q*, *Me*OC_6H_4); 51.8 (*q*, MeO(Pro)); 47.9, 47.5 (2*t*, 2 CH_2(δ))(Pro)); 28.2, 27.9 (2*t*, 2 CH_2(β)(Pro)); 25.8, 25.7 (2*t*, 2 CH_2(γ)(Pro)); 25.8, 25.0, 24.6, 24.6 (4*q*, 4 Me(Aib)). ESI-MS: 569 (45, $[M + K]^+$), 553 (100, $[M + Na]^+$), 531 (9, $[M + H]^+$), 402 (74, $[M - (Pro\text{-}OMe) + H]^+$), 317 (10, $[M - (Aib\text{-}Pro\text{-}OMe) + H]^+$), 220 (16, $[M - (Pro\text{-}Aib\text{-}Pro\text{-}OMe) + H]^+$), 183 (13, $C_9H_{15}N_2O_2^+$). Anal. calc. for $C_{27}H_{38}N_4O_7$ (530.62): C 61.12, H 7.22, N 10.56; found: C 59.77, H 7.51, N 9.99.

Suitable crystals of **18** for the X-ray crystal-structure determination were grown from $CHCl_3$ by slow evaporation of the solvent at r.t.

N-*(*N-*{*N-*[*N-*(4-Methoxybenzoyl)-2-methylalanyl]prolyl}-2-methylalanyl)proline* (p-*MeOBz-(Aib-Pro)$_2$-OH*; **19**). According to *GP 2*, **18** (100 mg, 0.188 mmol) in 10 ml of THF/MeOH/H_2O, LiOH·H_2O (32 mg, 0.752 mmol), stirring for 22 h: 95 mg (98%) of **19**. The isolated peptide acid was pure enough to be used in the next step without further purification. M.p. 138°. ^{1}H-NMR (CD_3OD): 8.61, 8.25 (2*s*, 2 NH); 8.01–7.98 (*m*, 2 arom. H); 7.14–7.11 (*m*, 2 arom. H); 4.64–4.59 (*dd*, *J* = 9.1, 8.3, CH(α)(Pro)); 4.56–4.52 (*dd*, *J* = 9.0, 8.5, CH(α)(Pro)); 3.97 (*s*, *Me*OC_6H_4); 3.94–3.88 (*m*, 1 H of CH_2(δ)(Pro)); 3.84–3.8 (*m*, 2 H of 2 CH_2(δ)(Pro)); 3.53–3.45 (*m*, 1 H of CH_2(δ)(Pro)); 2.33–2.12 (*m*, 2 CH_2(β)(Pro)); 2.10–1.77 (*m*, 2 CH_2(γ)(Pro)); 1.70, 1.69, 1.65, 1.63 (4*s*, 4 Me(Aib)). ^{13}C-NMR (CD_3OD): 175.9, 174.7, 174.2, 171.1 (4*s*, 4 C=O); 166.8 (*s*, Ar*C*=O); 164.2 (*s*, 1 arom. C); 130.4 (*d*, 2 arom. CH); 126.8 (*s*, 1 arom. C); 114.8 (*d*, 2 arom. CH); 63.6, 62.1 (2*d*, 2 CH(α)(Pro)); 58.2, 57.8 (2*s*, 2 C(α)(Aib)); 55.9 (*q*, *Me*OC_6H_4); 49.6, 49.1 (2*t*, 2 CH_2(δ)(Pro)); 29.6, 29.1 (2*t*, 2 CH_2(β)(Pro)); 26.7, 26.6 (2*t*, 2 CH_2(γ)(Pro)); 26.2, 25.4, 24.9, 24.6 (4*q*, 4 Me(Aib)). ESI-MS: 539 (11, $[M + Na]^+$), 517 (16, $[M + H]^+$), 402 (100, $[M - (Pro\text{-}OH) + H]^+$), 317 (19, $[M - (Aib\text{-}Pro\text{-}OH) + H]^+$), 220 (29, $[M - (Pro\text{-}Aib\text{-}Pro\text{-}OH) + H]^+$), 183 (22, $C_9H_5N_2O_2^+$).

N-*(*N-*[*N-*(*N-*{*N-*[*N-*(4-Methoxybenzoyl)-2-methylalanyl]prolyl}-2-methylalanyl)prolyl]-2-methylalanyl)proline Methyl Ester* (p-*MeOBz-(Aib-Pro)$_3$-OMe*; **20**). According to *GP 1*, **19** (95 mg, 0.184 mmol) in dry CH_2Cl_2 (5 ml) and **1b** (40 mg, 0.2024 mmol); stirring for 47 h, CC (CH_2Cl_2/MeOH from 150:1 to 10:1): 115 mg (88%) of **20**. M.p. 293° (dec.). IR: 3272*m*, 2953*w*, 2925*s*, 2854*w*, 1749*m*, 1639*s*, 1605*w*, 1542*m*, 1504*m*, 1467*m*, 1403*m*, 1377*w*, 1363*w*, 1318*w*, 1301*w*, 1255*m*, 1204*w*, 1178*m*, 1115*w*, 1094*w*, 1022*m*, 945*w*, 892*m*, 855*w*, 776*w*. ^{1}H-NMR: 8.04 (*s*, NH); 7.90–7.87 (*m*, 2 arom. H); 7.64, 7.57 (2*s*, 2 NH); 7.01–6.98 (*m*, 2 arom. H); 4.67–4.62 (*m*, CH(α)(Pro)); 4.63–4.57 (*m*, CH(α)(Pro)); 4.55–4.42 (*m*, CH(α)(Pro)); 3.94–3.90 (*m*, 2 H of 3 CH_2(δ)(Pro)); 3.87 (*s*, *Me*OC_6H_4); 3.85–3.77 (*m*, 2 H of 3 CH_2(δ)(Pro)); 3.65 (*s*, MeO(Pro)); 3.63–3.56 (*m*, 1 H of 3 CH_2(δ)(Pro)); 3.30–3.26 (*m*, 1 H of 3 CH_2(δ)(Pro)); 2.22–2.01 (*m*, 3 CH_2(β)(Pro)); 1.98–1.80 (*m*, 3 CH_2(γ)(Pro)); 1.64, 1.63, 1.58, 1.55, 1.50, 1.48 (6*s*, 6 Me(Aib)). ^{13}C-NMR: 173.4, 172.6, 172.5, 172.0 171.7, 171.6 (6*s*, 6 C=O); 166.5 (*s*, Ar*C*=O); 162.7 (*s*, 1 arom. C); 129.2 (*d*, 2 arom. CH); 125.1 (*s*, 1 arom. C); 113.9 (*d*, 2 arom. CH); 62.4, 62.2, 60.5 (3*d*, 3 CH(α)(Pro)); 57.1, 56.5, 56.4 (3*s*, 3 C(α)(Aib)); 55.4 (*q*, *Me*OC_6H_4); 51.7 (*q*, MeO(Pro)); 48.2, 47.9, 47.7 (3*t*, 3 CH_2(δ))(Pro)); 28.9, 28.6, 27.9 (3*t*, 3 CH_2(β)(Pro)); 26.2, 25.8, 25.5 (3*t*, 3 CH_2(γ)(Pro)); 25.8, 25.7, 25.0, 24.6, 24.5, 24.0 (6*q*, 6 Me(Aib)). ESI-MS: 751 (9, $[M + K]^+$), 735 (25, $[M + Na]^+$), 713 (25, $[M + H]^+$) 584 (100, $[M - (Pro\text{-}OMe) + H]^+$), 402 (13). Anal. calc. for $C_{36}H_{52}N_6O_9$ (712.85): C 60.66, H 7.35, N 11.79; found: C 60.56, H 7.54, N 11.49.

5. *Solvent and Temperature Dependence of the Chemical Shifts of the NH Groups.* The peptides **11**, **13**–**15**, and **18** were dissolved in $CDCl_3$ (*ca.* 0.2M), and the chemical shifts of the NH groups were determined at *ca.* 30°. Then, using a syringe, 2, 4, 6, 8, 10, and 12% (*v*/*v*) of (D_6)DMSO were added, and, after each addition, the chemical shifts were determined again. For the determination of the temp. dependence, the NH absorption in $CDCl_3$ soln. (*ca.* 0.2M), was recorded between 265 and 314 K in intervals of 7 K.

6. *X-Ray Crystal-Structure Determinations of* **11**, **14**, **15**, *and* **18** (see *Table 12*, and *Figs. 2–9*)[3]). The measurements for compounds **11** and **18** were conducted on a *Rigaku AFC5R* diffractometer using graphite-monochromated MoK_α radiation (λ = 0.71073 Å) and a 12-kW rotating anode generator, while those for compounds **14** and **15** were performed on a *Nonius KappaCCD* area-detector diffractometer [20] using graphite-monochromated MoK_α radiation (λ = 0.71073 Å) and an *Oxford Cryosystems Cryostream 700* cooler. Data reduction for **14** and **15** was accomplished with *HKL Denzo* and *Scalepack* [21]. The intensities were corrected for *Lorentz* and polarization effects. A numerical absorption correction [22] was applied in the case of **15**, an empirical absorption correction based on azimuthal scans of several reflections [23] was applied for **11**, and an absorption correction based on the multi-scan method [24] was applied in the case of **14**. No absorption correction was applied in the case of **18**. In all cases, equivalent reflections, other than *Friedel* pairs, were merged. Data collection and refinement

[3]) CCDC-869148–869151 contain the supplementary crystallographic data for this article. These data can be obtained free of charge from *The Cambridge Crystallographic Data Centre via* www.ccdc.cam.ac.uk/data_request/cif.

Table 12. *Crystallographic Data for Compounds* **11**, **14**, **15**, *and* **18**

	11	**14**	**15**	**18**
Crystallized from	CH_2Cl_2/AcOEt	CH_2Cl_2	CH_2Cl_2/AcOEt/hexane	$CHCl_3/CH_2Cl_2$/AcOEt
Empirical formula	$C_{35}H_{49}BrN_6O_8 \cdot 0.25\ CH_2Cl_2$	$C_{31}H_{46}BrN_5O_5 \cdot 2\ CH_2Cl_2$	$C_{49}H_{74}BrN_9O_9$	$C_{27}H_{38}N_4O_7 \cdot CH_2Cl_2 \cdot 0.25\ H_2O$
Formula weight	782.49	815.50	1013.08	620.05
Crystal color, habit	colorless, prism	colorless, prism	colorless, prism	colorless, prism
Crystal dimensions [mm]	$0.25 \times 0.30 \times 0.45$	$0.08 \times 0.20 \times 0.25$	$0.10 \times 0.17 \times 0.30$	$0.20 \times 0.28 \times 0.48$
Temp. [K]	173(1)	160(1)	160(1)	173(1)
Crystal system	orthorhombic	orthorhombic	monoclinic	orthorhombic
Space group	$P2_12_12_1$	$P2_12_12_1$	$P2_1$	$P2_12_12_1$
Z	4	4	2	4
Reflections for cell determination	25	87797	58710	25
2θ Range for cell determination [°]	26–35	4–55	4–50	22–35
Unit cell parameters a [Å]	20.236(3)	9.4174(1)	16.4931(2)	13.879(3)
b [Å]	22.521(4)	19.1461(2)	9.4164(1)	22.758(3)
c [Å]	9.552(3)	21.6971(2)	17.4769(3)	9.953(3)
β [°]	90	90	104.0990(5)	90
V [Å^3]	4353(1)	3912.13(7)	2632.50(6)	3143.5(14)
D_x [g cm^{-3}]	1.195	1.390	1.278	1.310
$\mu(\mathrm{Mo}K_\alpha)$ [mm^{-1}]	1.028	0.371	0.844	0.256
Scan type	$\omega/2\theta$	ϕ and ω	ϕ and ω	$\omega/2\theta$
$2\theta_{(\max)}$ [°]	50	55	50	55
Transmission factors [min; max]	0.833; 1.000	0.843; 0.919	0.803; 0.893	–
Total reflections measured	7129	111819	57957	4707
Symmetry independent reflections	6368	8978	9269	4573
Reflections with $I > 2\sigma(I)$	4074	6380	8383	2770
Reflections used in refinement	6346	8972	9267	4571
Parameters refined; restraints	460; 0	490; 52	622; 1	421; 0
Final $R(F)$ [$I > 2\sigma(I)$ reflections]	0.0616	0.0286	0.0673	0.0546
$wR(F^2)$ (all data)	0.1677	0.0627	0.1994	0.1587
Weighting parameters [a; b][a])	0.0946; 0	0; 0	0.1346; 2.2146	0.0666; 0.5926
Goodness of fit	1.001	0.621	1.053	1.027
Secondary extinction coefficient	0.0028(6)	0.0021(2)	–	–
Absolute structure parameter	0.041(14)	–0.014(4)	0.011(12)	0.3(2)
Final $\Delta_{\max}/\sigma$	< 0.001	0.008	0.001	0.001
$\Delta\rho$(max; min) [e Å^{-3}]	0.48; -0.68	0.33; -0.29	1.71; -1.09	0.23; -0.24

[a]) $w^{-1} = \sigma^2(F_o^2) + (aP)^2 + bP$ where $P = (F_o^2 + 2F_c^2)/3$.

parameters are compiled in *Table 12*. The structures were solved by direct methods using either *SIR92* [25] or *SHELXS97* [26].

The crystal lattice of **11** contains highly disordered or diffuse solvent molecules. An analysis of the residual electron-density peaks suggests that partially occupied sites for CH_2Cl_2 molecules are present, but it was not possible to adequately model their contribution to the overall structure in any logical manner. Therefore, the *SQUEEZE* routine [27] of the program *PLATON* [28] was employed. The procedure gave satisfactory *R* factors for the refinement and suitable geometric parameters for the peptide molecule, and there were no significant peaks of residual electron density to be found in the voids of the structure. The solvent molecules occupy a total volume of 866 Å^3 per unit cell, divided into two symmetry-related regions. The electron count in the solvent region was calculated to be 42 e per unit cell. This corresponds with the presence of a total of one CH_2Cl_2 molecule per unit cell, but spread across two symmetry-related sites. For the purposes of the calculation of the formula weight, density, F(000), and the linear absorption coefficient, it was assumed that the ratio of peptide **11** to CH_2Cl_2 in the structure is 4 : 1.

The asymmetric unit of **14** contains one peptide and two CH_2Cl_2 molecules, one of which is highly disordered. Three partially occupied sets of positions were defined for the Cl-atoms of the disordered solvent molecule, and the total occupancies of the sets of atoms were restrained to sum to 1.0. Similarity restraints were applied to the C–Cl bond lengths, while neighboring atoms within and between each orientation of the disordered CH_2Cl_2 molecules were restrained to have similar and pseudo-isotropic atomic displacement parameters.

In the case of **18**, the asymmetric unit contains one peptide and one highly disordered CH_2Cl_2 molecule plus a site for a H_2O molecule which is only one quarter occupied. Two equally occupied positions were defined for each of the Cl-atoms of the CH_2Cl_2 molecule, but the large values for their atomic displacement ellipsoids suggest that this molecule is even more highly disordered within its cavity. The H_2O molecule site is actually very close to that of the CH_2Cl_2 molecule, and it is possible that either the H_2O molecule is disordered with the CH_2Cl_2 molecule, or there is no H_2O at all, and that the electron density that has been assigned to the H_2O O-atom actually represents another low occupancy disordered position for an atom of the CH_2Cl_2 molecule. However, the refined model appears to provide the best match with the electron density in the solvent region. The central five-membered ring of the peptide molecule has a disordered envelope conformation in which the envelope flap atom, C(26), is flipped alternately to both sides of the ring. The major conformation of this ring occurs in 56(2)% of the molecules. The other five-membered ring also shows slight evidence for similar disorder involving C(31), but a disordered model could not be refined satisfactorily.

For all structures, the non-H atoms were refined anisotropically. The amide H-atoms of **14** and **18** were located in a difference electron density map, and their positions were allowed to refine together with individual isotropic displacement parameters. The H-atoms of the CH_2Cl_2 and H_2O solvent molecules of **18** were not included in the model. All of the remaining H-atoms in each structure were placed in geometrically calculated positions and refined using a riding model where each H-atom was assigned a fixed isotropic displacement parameter with a value equal to 1.2 U_{eq} of its parent C-atom (1.5U_{eq} for the Me groups). The refinement of each structure was carried out on F^2 using full-matrix least-squares procedures [26], which minimized the function $\Sigma w(F_o^2 - F_c^2)^2$. Corrections for secondary extinction were applied for **11** and **14**. Between two and four reflections whose intensities were considered as outliers were omitted from the final refinement of each structure. Refinement of the absolute structure parameter [29] confidently confirmed that the refined model represents the true enantiomorph for **11**, **14**, and **15** (*Table 12*), which is consistent with the peptide configurations expected from the synthesis. The absolute structure for **18** could not be determined owing to the weak anomalous scattering of the material. The enantiomer used in the refinement was based on the known (*S*)-configuration at C(5) and C(11).

Neutral atom scattering factors for non-H-atoms were taken from [30a], and the scattering factors for H-atoms were taken from [31]. Anomalous dispersion effects were included in F_c [32]; the values for f' and f'' were those of [30b]. The values of the mass attenuation coefficients are those of [30c]. All calculations were performed using the *SHELXL97* [26] program.

REFERENCES

[1] S. Stoykova, A. Linden, H. Heimgartner, *Chimia* **2001**, *55*, 627.
[2] J. C. Pandey, J. C. Cook Jr., K. L. Rinehart Jr., *J. Am. Chem. Soc.* **1977**, *99*, 8469.
[3] 'Peptaibiotics', Eds. C. Toniolo, H. Brückner, Verlag Helvetica Chimica Acta, Zürich, 2009.
[4] a) I. L. Karle, J. Flippen-Anderson, M. Sukumar, P. Balaram, *Proc. Natl. Acad. Sci. U.S.A.* **1987**, *84*, 5087; b) I. L. Karle, P. Balaram, *Biochemistry* **1990**, *29*, 6747; c) C. Toniolo, E. Benedetti, *Trends Biochem. Sci.* **1991**, *16*, 350; d) E. Benedetti, B. Di Blasio, V. Pavone, C. Pedone, C. Toniolo, M. Crisma, *Biopolymers* **1992**, *32*, 453; e) A. Szekeres, B. Leitgeb, L. Kredics, Z. Antal, L. Hatvani, L. Manczinger, C. Vágvölgyi, *Acta Microbiol. Immunol. Hung.* **2005**, *52*, 137; f) M. Crisma, F. Formaggio, A. Moretto, C. Toniolo, *Biopolymers* **2006**, *84*, 3.
[5] a) Y. V. Venkatachalapathi, P. Balaram, *Biopolymers* **1981**, *20*, 1137; b) V. Moretto, G. Valle, M. Crisma, G. M. Bonora, C. Toniolo, *Int. J. Biol. Macromol.* **1992**, *14*, 178; c) B. Di Blasio, V. Pavone, M. Saviano, A. Lombardi, F. Nastri, C. Pedone, E. Benedetti, M. Crisma, M. Anzolin, C. Toniolo, *J. Am. Chem. Soc.* **1992**, *114*, 6273; d) G. Yoder, T. A. Keiderling, F. Formaggio, M. Crisma, C. Toniolo, *Biopolymers* **1995**, *35*, 103; e) I. Ségalas, Y. Prigent, D. Davoust, B. Bodo, S. Rebuffat, *Biopolymers* **1999**, *50*, 71; f) M. Crisma, G. Valle, G. M. Bonora, C. Toniolo, G. Cavicchioni, *Int. J. Pept. Protein Res.* **1993**, *41*, 553; g) C. Tomasini, G. Luppi, M. Monar, *J. Am. Chem. Soc.* **2006**, *128*, 2410.
[6] P. Balaram, K. Krishna, M. Sukumar, I. R. Mellor, M. S. P. Sanson, *Eur. Biophys. J.* **1992**, *21*, 117; M. S. P. Sansom, P. Balaram, I. L. Karle, *Eur. Biophys. J.* **1992**, *21*, 369; M. S. P. Sansom, *Eur. Biophys. J.* **1993**, *22*, 105; L. Béven, D. Duval, S. Rebuffat, F. G. Ridell, B. Bodo, H. Wróblewski, *Biochem. Biophys. Acta – Biomembranes* **1998**, *1372*, 78; J. K. Chugh, B. A. Wallace, *Biochem. Soc. Trans.* **2001**, *29*, 565; T. P. Galbraith, R. Harris, P. C. Driscoli, B. A. Wallace, *Biophys. J.* **2003**, *84*, 185; A. O. O'Reilly, B. A. Wallace, *J. Pept. Sci.* **2003**, *9*, 769; H. Duclohier, *Eur. Biophys. J.* **2004**, *33*, 169; L. Whitemore, B. A. Wallace, *Eur. Biophys. J.* **2004**, *33*, 233; Z. O. Shenkarev, T. A. Balashova, Z. A. Yakimenko, T. V. Ovchinnikova, A. S. Arseniev, *Biophys. J.* **2004**, *86*, 3687; R. Gessmann, D. Axford, R. L. Owen, H. Brückner, K. Petratos, *Acta Crystallogr., Sect. D* **2012**, *68*, 109.
[7] H. Heimgartner, *Angew. Chem., Int. Ed.* **1991**, *30*, 238.
[8] a) P. Wipf, H. Heimgartner, *Helv. Chim. Acta* **1990**, *73*, 13; b) R. Luykx, C. B. Bucher, A. Linden, H. Heimgartner, *Helv. Chim. Acta* **1996**, *79*, 527; c) C. B. Bucher, H. Heimgartner, *Helv. Chim. Acta* **1996**, *79*, 1903; d) N. Pradeille, H. Heimgartner, *J. Pept. Sci.* **2003**, *9*, 827; e) R. T. N. Luykx, A. Linden, H. Heimgartner, *Helv. Chim. Acta* **2003**, *86*, 4093; f) N. Pradeille, O. Zerbe, K. Möhle, A. Linden, H. Heimgartner, *Chem. Biodiversity* **2005**, *2*, 1127; g) A. Linden, N. Pradeille, H. Heimgartner, *Acta Crystallogr., Sect. C* **2006**, *62*, o249; h) S. Stamm, H. Heimgartner, *Tetrahedron* **2006**, *62*, 9671; i) W. Altherr, A. Linden, H. Heimgartner, *Chem. Biodiversity* **2007**, *4*, 1144.
[9] C. B. Bucher, A. Linden, H. Heimgartner, *Helv. Chim. Acta* **1995**, *78*, 935; K. N. Koch, G. Hopp, A. Linden, K. Moehle, H. Heimgartner, *Helv. Chim. Acta* **2001**, *84*, 502; K. N. Koch, A. Linden, H. Heimgartner, *Tetrahedron* **2001**, *57*, 2311; K. A. Brun, A. Linden, H. Heimgartner, *Helv. Chim. Acta* **2001**, *84*, 1756; K. A. Brun, A. Linden, H. Heimgartner, *Helv. Chim. Acta* **2002**, *85*, 3422; T. Jeremic, A. Linden, H. Heimgartner, *Chem. Biodiversity* **2004**, *1*, 1730; T. Jeremic, A. Linden, H. Heimgartner, *Helv. Chim. Acta* **2004**, *87*, 3056; T. Jeremic, A. Linden, K. Moehle, H. Heimgartner, *Tetrahedron* **2005**, *61*, 1871; K. A. Brun, A. Linden, H. Heimgartner, *Helv. Chim. Acta* **2008**, *91*, 526; T. Jeremic, A. Linden, H. Heimgartner, *J. Pept. Sci.* **2008**, *14*, 1051; I. Dannecker-Dörig, A. Linden, H. Heimgartner, *Coll. Czech. Chem. Commun.* **2009**, *74*, 901; I. Dannecker-Dörig, A. Linden, H. Heimgartner, *Helv. Chim. Acta* **2011**, *94*, 993.
[10] S. Stamm, A. Linden, H. Heimgartner, *Helv. Chim. Acta* **2003**, *86*, 1371; S. Stamm, H. Heimgartner, *Eur. J. Org. Chem.* **2004**, 3820; S. Stamm, A. Linden, H. Heimgartner, *Helv. Chim. Acta* **2006**, *89*, 1.
[11] R. A. Breitenmoser, T. R. Hirt, R. T. N. Luykx, H. Heimgartner, *Helv. Chim. Acta* **2001**, *84*, 972.
[12] J. Bernstein, R. E. Davis, L. Shimoni, N.-L. Chang, *Angew. Chem., Int. Ed.* **1995**, *34*, 1555.
[13] C. K. Johnson, 'ORTEP II', Report ORNL-5138, Oak Ridge National Laboratory, Oak Ridge, Tennessee, 1976.
[14] P. Chakrabarti, S. Chakrabarti, *J. Mol. Biol.* **1998**, *284*, 867.
[15] B. V. Venkataraman Prasad, P. Balaram, *Int. J. Biol. Macromol.* **1982**, *4*, 99.

[16] H. Kessler, *Angew. Chem., Int. Ed.* **1982**, *21*, 512.
[17] M. Crisma, M. Anzolin, G. M. Bonora, C. Toniolo, E. Benedetti, B. Di Blasio, V. Pavone, M. Saviano, A. Lombardi, F. Nastri, C. Pedone, *Gazz. Chim. Ital.* **1992**, *122*, 239.
[18] C. Toniolo, E. Benedetti, C. Pedone, *Gazz. Chim. Ital.* **1986**, *116*, 355.
[19] B. V. Venkataraman Prasad, P. Balaram, *Biopolymers* **1981**, *20*, 625.
[20] R. Hooft, KappaCCD Collect Software, Nonius BV, Delft, The Netherlands, 1999.
[21] Z. Otwinowski, W. Minor, in 'Methods in Enzymology', Vol. 276, 'Macromolecular Crystallography', Part A, Eds. C. W. Carter Jr., R. M. Sweet, Academic Press, New York, 1997, p. 307.
[22] P. Coppens, L. Leiserowitz, D. Rabinovich, *Acta Crystallogr.* **1965**, *18*, 1035.
[23] A. C. T. North, D. C. Phillips, F. S. Mathews, *Acta Crystallogr., Sect. A* **1968**, *24*, 351.
[24] R. H. Blessing, *Acta Crystallogr., Sect. A* **1995**, *51*, 33.
[25] A. Altomare, G. Cascarano, C. Giacovazzo, A. Guagliardi, M. C. Burla, G. Polidori, M. Camalli, *SIR92*, *J. Appl. Crystallogr.* **1994**, *27*, 435.
[26] G. M. Sheldrick, *Acta Crystallogr., Sect. A* **2008**, *64*, 112.
[27] P. van der Sluis, A. L. Spek, *Acta Crystallogr., Sect. A* **1990**, *46*, 194.
[28] A. L. Spek, *Acta Crystallogr., Sect. D* **2009**, *65*, 148.
[29] H. D. Flack, *Acta Crystallogr., Sect. A* **1983**, *39*, 876–881; G. Bernardinelli, H. D. Flack, *Acta Crystallogr., Sect. A* **1985**, *41*, 500–511.
[30] a) E. N. Maslen, A. G. Fox, M. A. O'Keefe, in 'International Tables for Crystallography', Ed. A. J. C. Wilson, Kluwer Academic Publishers, Dordrecht, 1992, Vol. C, Table 6.1.1.1, p. 477; b) D. C. Creagh, W. J. McAuley, in 'International Tables for Crystallography', Ed. A. J. C. Wilson, Kluwer Academic Publishers, Dordrecht, 1992, Vol. C, Table 4.2.6.8, p. 219; c) D. C. Creagh, J. H. Hubbell, in 'International Tables for Crystallography', Ed. A. J. C. Wilson, Kluwer Academic Publishers, Dordrecht, 1992, Vol. C, Table 4.2.4.3, p. 200.
[31] R. F. Stewart, E. R. Davidson, W. T. Simpson, *J. Chem. Phys.* **1965**, *42*, 3175.
[32] J. A. Ibers, W. C. Hamilton, *Acta Crystallogr.* **1964**, *17*, 781.

Received March 20, 2012